

IRON-SULFUR PROTEIN MATURATION IN STAPHYLOCOCCUS AUREUS: THE  
PROTEIN YLAN HAS A ROLE IN IRON HOMEOSTASIS

By

MARY ELIZABETH FOLEY

A thesis submitted to the

School of Graduate Studies

Rutgers, The State University of New Jersey

In partial fulfilment of the requirements

For the degree of

Master of Science

Graduate Program in Microbial Biology

Written under the direction of

Jeffrey Boyd

And approved by

---

---

---

New Brunswick, New Jersey

October 2018

## ABSTRACT OF THE THESIS

Iron-Sulfur protein maturation in *Staphylococcus aureus*: The protein YlaN has a role in iron homeostasis

By MARY ELIZABETH FOLEY

Thesis Director:

Jeffrey Boyd

Iron-sulfur (FeS) cluster containing proteins are essential to fundamental cellular processes like central metabolism and respiration. Organisms unable to make FeS clusters show metabolic abnormalities such as amino acid auxotrophies, poor growth when Fe is limiting, and resistance to certain antibiotics. *Bacillus subtilis* strains lacking *ylaN* show similar phenotypes, therefore we tested the hypothesis that the protein YlaN functions in the maturation of FeS proteins. Our results showed that a *Staphylococcus aureus* strain lacking *ylaN* displayed reduced growth in iron-limited media and when grown in the presence of the divalent metal chelator 2,2'-dipyridyl. The  $\Delta$ *ylaN* strain grew better than wild-type in the presence of streptonigrin, which is an antibiotic that requires Fe for killing. The  $\Delta$ *ylaN* strain also had decreased activity of the FeS cluster dependent enzyme aconitase. Purified YlaN prevented free Fe from binding to 1,10-phenanthroline. Taken together, these results show that YlaN has a role in regulating free Fe in *S. aureus* which is important in the maturation of FeS proteins.

## ACKNOWLEDGEMENTS

Jeff Boyd, thank you for giving me the opportunity to perform research in your lab. Thank you for showing me how to build strains, purify proteins, perform many of the assays, and for your guidance and advice. Thank you for always making time to answer the many questions I had concerning this project. Hassan Al-Tameemi, thank you for showing me how to spot plates and yeast clone, and for helping me change almost all of the tanks for the anaerobic chamber. Also, thank you for your sense of humor and kindness, for putting up with my taste in music, and for rescuing me when I locked myself out of the office (on more than one occasion). Thank you, Gerben Zylstra, for being a good listener, a great teacher, and for answering all of my questions regarding graduate school. Max Häggblom, Ines Rauschenbach, Ramadalis Keddis, and Jessica Lisa, thank you all for being wonderful instructors and TA supervisors; your knowledge and enthusiasm for education are awesome, and I hope I can mirror it someday. Finally, I'd like to thank the other microbial biology graduate students at Rutgers. Your friendship and encouragement over the last two years helped me get to this point, and it will be remembered for the rest of my life.

## TABLE OF CONTENTS

Abstract.....	ii
Acknowledgments.....	iii
Table of Contents.....	iv
List of Tables.....	v
List of Figures and Illustrations.....	vi
Introduction.....	1
Methods.....	4
Results.....	12
Discussion.....	18
References.....	41

## LIST OF TABLES

Primer Table (ref. p 4) .....	24
Strain Table (ref. p 5) .....	25
Plasmid Table (ref. p 5) .....	26
Trace Minerals Solution Table (ref. p 8) .....	26

## LIST OF FIGURES

Figure 1: Growth in the presence and absence of 2,2-dipyridyl (ref. p 12) .....	27
Figure 2: Growth in Fe deplete media with and without supplemented Fe (ref. p 13) .....	28
Figure 3: Aconitase activity of <i>ΔylaN</i> , (ref. p 14, 15) .....	29
Figure 4: Aconitase activity of <i>ΔylaN</i> with complementation (ref. p 13, 16) .....	30
Figure 5: Growth of <i>ΔylaN</i> treated with streptonigrin ( ref. p 14) .....	31
Figure 6: Survival after treatment with hydrogen peroxide (ref. p 15) .....	32
Figure 7: Growth in the presence of methyl viologen (ref. p 15, 16) .....	33
Figure 8: Sequence alignments of YlaN, YlaN <sub>C38A</sub> variant, and YlaN homologs (ref. p 16, 21) .....	34
Figure 9: Protein structure of YlaN homodimer (ref. p 16) .....	35
Figure 10: Identified domains of YlaN (ref. p 16, 22).....	36
Figure 11: Maximum likelihood tree for YlaN homologs (ref. p 16, 22) .....	37
Figure 12: Fe competition between YlaN and 1,10-phenanthroline (ref. p 17) .....	38
Figure 13: Fe competition between YlaN and MagFura-2 (ref p 17, 18) .....	39

## Introduction

Iron is essential in almost all living organisms. It is one of the most abundant elements on earth (Yaroshevsky, 2006). It is present in deep-sea hydrothermal vents in the form of pyrite ( $\text{FeS}_2$ ) and is thought to be important in the development of the first carbon fixation pathway according to the chemoautotrophic origin of life theory (Huber and Wächtershäuser, 1997). Iron acts as a cofactor to many proteins. It can be bound by itself, as in the case of non-heme mononuclear (Peck and van der Donk, 2017) and dinuclear iron-dependent enzymes (Frey et al., 2014). It can also be bound as part of a prosthetic group like in heme and in iron-sulfur ( $\text{FeS}$ ) cluster containing proteins. Because iron is a necessity for almost all bacterial infections, host immune systems have developed various ways of limiting the iron available to pathogens. This includes hypoferremia and free-iron sequestration by glycoproteins (reviewed in Cassat and Skaar, 2013).

Although iron is abundant in the natural environment, it is mostly present as  $\text{Fe}^{3+}$ , which has low solubility. In living tissue, it is usually bound by heme or ferritin (reviewed in Skaar, 2010). This inaccessibility makes it a limiting reagent in many cellular processes. Over time, bacteria have evolved iron uptake systems which can overcome this challenge. Iron chelators, like enterochelin (Williams and Carbonetti, 1986), can solubilize  $\text{Fe}^{3+}$  outside of the cell and transport it back into the cell through siderophore specific outer membrane receptors (gram-negative) or ABC permeases (gram-positive) (reviewed in Andrews et al., 2003). The iron is kept in iron storage proteins and is later made available when the extracellular iron is depleted (Laulhère et al., 1992; Yasmin et al., 2011).

Superoxide ( $\text{O}_2^-$ ) and hydrogen peroxide ( $\text{H}_2\text{O}_2$ ) are both unintended byproducts of oxidative respiration. Free  $\text{Fe}^{2+}$  and  $\text{Fe}^{3+}$  in the cell will react with  $\text{H}_2\text{O}_2$  to produce  $\text{OH}^\bullet$  and  $\text{OOH}^\bullet$ , respectively, via Fenton chemistry (reviewed in Chemizmu and Fentona, 2009). These

hydroxyl radicals are highly reactive and cause cellular damage by oxidizing DNA and amino acids (Keyer and Imlay, 1996; Català et al., 2000). FeS cluster cofactors are also a target of ROS. The aconitase enzyme contains a solvent-exposed FeS cluster that can be oxidized from a  $[\text{Fe}_4\text{S}_4]$  to a  $[\text{Fe}_3\text{S}_4]^{+1}$  state, which results in the loss of enzyme activity and increased cytosolic  $\text{Fe}^{2+}$  (Jang and Imlay, 2007). Thus, it is important to limit the amount of “free” or non-chelated iron available inside the cell, especially in aerobically respiring cells.

Organisms control iron homeostasis through gene regulators such as Fur (Ferric Uptake Regulator) and DxtR. Regulation by Fur is used by gram-negative bacteria and by gram-positive bacteria with a low GC content (reviewed in Hantke, 2001). When iron is in high quantity inside the cell, it binds to Fur, which then acts as a co-repressor. Iron-bound Fur binds to DNA and depresses the expression of iron chelators and iron import proteins. This in turn decreases iron uptake by the cell (Hantke, 1981). Under high iron conditions, Fur, along with PerR, positively controls the expression of catalase (Horsburgh et al., 2001), a protein that breaks down  $\text{H}_2\text{O}_2$  into water and dioxygen, providing the cell protection against oxidation. Aconitase also acts to regulate iron storage inside the cell. Under low iron conditions, apo-aconitase functions as an RNA binding molecule and ultimately blocks the formation of ferritin (an iron storage protein) and stabilizes the mRNAs for Fe uptake (Hurling et al., 1994).

FeS cluster containing proteins have a variety of functions inside the cell including redox reactions, acid-base chemistry, and environmental sensing (reviewed in Beinert, 1997; Lill, 2009). FeS clusters can form spontaneously in vitro (Hong, 1969), however, inside the cell their assembly is controlled as to limit free iron and sulfur. Three FeS cluster biosynthesis pathways have been described in bacteria: ISC (*Iron-Sulfur Cluster*), NIF (*Nitrogen Fixation*), and SUF (*Sulfur Mobilization*). Each pathway contains unique proteins for FeS cluster maturation, but the method of assembly has been conserved among the systems. A cysteine desulfurase enzyme takes sulfur atoms from cysteine and donates them to a scaffold protein where they bind with  $\text{Fe}^{2+}$



forming the cluster. Then the FeS cluster is either directly introduced into its ascribed protein, or it is transported to a protein for insertion by an FeS cluster chaperone.

The SUF pathway is the most widely distributed among bacteria, and the only system thought to be used by gram-positive bacteria (Boyd et al., 2014). In SUF-directed FeS cluster formation, the sulfurtransferase (SufU) receives persulfide from the desulfurase (SufS) and transfers  $S^0$  to the scaffold proteins (SufBCD). SufA and Nfu are FeS carrier proteins. SufT and the low-molecular-weight thiol BSH have yet undefined roles in the maturation of FeS proteins (Rosario-Cruz et al., 2015; Mashruwala et al., 2015). Currently, the electron and  $Fe^{2+}$  donors are unknown.

YlaN is an essential protein in the gram-positive bacterium *Bacillus subtilis* (Peters et al., 2016). YlaN depletion in *B. subtilis* results in defects in cell wall synthesis, and sensitivity to growth in the presence of the divalent metal chelator 2,2'-dipyridyl (DIP). Interestingly, these phenotypes are shared with strains that are depleted in *SufBCDSU*. These findings led us to hypothesize that YlaN functions in the maturation of FeS proteins.

*B. subtilis* utilizes the FeS proteins IspH and IspG to synthesize essential isoprenoids via the deoxyxylulose 5-phosphate (DXP) pathway (Wang and Oldfield, 2014; Wagner et al., 2000). When this pathway is replaced with the melevonate pathway of isoprenoid synthesis, which does not rely on FeS proteins, *sufBCDSU* deletions are no longer lethal in *B. subtilis* (Tanka et al., 2016; Yoykoama et al., 2018), meaning the inability of *SufBCDSU* mutants to mature IspH and IspG is what leads to cell death. Peters et al. (2016) showed that *B. subtilis* strains depleted in *sufBCDSU*, genes needed for isoprenoid synthesis, or *ylaN*, showed resistance to cell-wall targeting antibiotics, which also points to a possible role of YlaN in the maturation of FeS proteins. The gram-positive bacterium *Staphylococcus aureus* uses the melevonate pathway to make isoprenoids (Horbach et al., 1993). This could mean that *ylaN* is not an essential gene in *S. aureus*, which would make it an ideal organism with which to study the function of YlaN.

*S. aureus* is an opportunistic pathogen that is carried by at least 30% of the population, usually on the skin or in the throat or sinus cavity (Kuehnert et al., 2006). *S. aureus* infections usually present as treatable skin infections; however, more serious forms of infection can occur. These often-fatal infections include necrotizing fasciitis, necrotizing pneumonia, infective endocarditis, and toxic-shock syndrome (Miller et al., 2005; Tong et al., 2015; Barbour et al., 1984). Difficulties in treating *S. aureus* infections have arisen due to the increase in antibiotic resistance strains like MRSA and VRSA. Because the system used to build FeS clusters in *S. aureus* is different from the pathways used in humans, the SUF system could be used as a target for new antibiotic development (Lill, 2009). Importantly, the system used to build FeS clusters is essential in *S. aureus*. Recent research has shown that defects in the SUF system alter the virulence of *S. aureus* (Roberts et al., 2017; Choby et al., 2016).

The purpose of my research thesis is to test the hypothesis that YlaN is involved in FeS cluster synthesis in *S. aureus*. We created a *ylaN* mutant strain and showed that it was not essential in *S. aureus*. The *ylaN* mutant strain showed similar phenotypes to strains lacking genes needed for FeS biogenesis under low iron conditions. Improved growth, when compared to wildtype (WT), was seen when the *ylaN* mutant was exposed to H<sub>2</sub>O<sub>2</sub> and streptonigrin. Purified YlaN was able to inhibit 1,10-phenanthroline from binding iron. Together, these results suggest that YlaN is important in Fe homeostasis inside the cell.

## Methods

### Materials

Primers were purchased from Integrated DNA Technologies and are listed in **Table 1**. Quick-Load® 1 kb Extend DNA Ladder, dNTP solution mix, Phusion DNA polymerase, restriction enzymes, quick DNA ligase, and associated reaction buffers were purchased from New

England Biolabs. Plasmid mini-prep and gel extraction kits were purchased from Qiagen.

Lysostaphin was purchased from Ambi Products. Electro-competent and chemically-competent

*Escherichia coli* PX5- $\alpha$  cells were ordered from Protein Express. Pierce BCA Solid and DNase

were purchased from Thermo Fisher Scientific. Salmon Sperm was purchased from Ambion.

Tryptic Soy Broth (TSB), Luria Broth (LB), agar powder, Methyl Viologen Hydrate, and

Dithiothreitol (DTT) were purchased from Fischer Scientific. Chelex® 100 chelating agent was

ordered from BioRad. MagFur-2 tetrasodium salt was ordered from Biotium. All other chemicals

were purchased from Sigma-Aldrich unless noted otherwise.

### Growth Conditions

If not specifically stated, the conditions used to culture the cells are as followed: *S. aureus* cells were aerobically grown in TSB in either 10 mL or 25 mL tubes with a headspace to culture medium volume ratio of 5. DifcoBioTech agar was added at 1.5% w/v for solid medium. Incubation occurred at 37°C, with shaking at 200 rpm for broth cultures. Unless noted otherwise, all *S. aureus* strains (**Table 2**) used in this study were constructed using USA300 LAC, which is a community associated methicillin-resistant strain that is lacking the plasmid (pUSA03) that provides resistance to erythromycin (Boles et al., 2010). Plasmids were retained by antibiotic selection with the following concentrations: 150  $\mu$ g/mL ampicillin (Amp); 30  $\mu$ g/mL chloramphenicol (Cm); 10  $\mu$ g/mL erythromycin (Erm); 3  $\mu$ g/mL tetracycline. The types of plasmids that were used to build the strains used in this study are listed in **Table 3**.

### Transformations and Transductions

Constructed plasmids were hosted in *Escherichia coli* PX5- $\alpha$ . Clones were transformed into *S. aureus* strain RN4220 (Kreiwirth et al., 1983). Movement of clones between *S. aureus* strains was performed by transduction using bacteriophage 80 $\alpha$ . All *S. aureus* mutant strains and

plasmids were verified using PCR, or by DNA sequencing performed by Genewiz, in South Plainfield, NJ.

#### Plasmid and Strain Building

**Protein Expression Vector pGEX\_ylaN:** Strain JMB1100 was used as the template for all strains unless otherwise noted. *ylaN* was amplified using forward primer ylaNGSTBamHI and reverse primer ylaN3XhoI. The PCR product includes the start codon and ends immediately after *ylaN*, with complementary plasmid nucleotides on both ends. The pGEX\_GPI plasmid was purified from an overnight culture of strain JMB7588. The plasmid and the PCR product were digested with XhoI and BamHI and purified by gel extraction. The purified digests were ligated together and then transformed into chemically competent PH5- $\alpha$  cells.

**Multicopy Complementary Vector pEPSA\_ylaN:** *ylaN* was amplified using forward primer pEPSylaNforYC and reverse primer pEPylaNrevYC which amplified 15bp upstream from the start codon to 50bp downstream of the end of *ylaN*. The pEPSA\_YCC plasmid template was purified from an overnight culture of strain JMB7751. The plasmid was digested with SalI and MluI and purified via gel extraction. The digested plasmid and the PCR product were combined into a vector through homologous recombination in yeast following the protocol by Joska et al. (2014). pEPSA contains a ribosomal binding site for *sodA* which is induced by xylose (Forsyth et al., 2002).

**Complementation Vector pCM28\_ylaN:** The same method used to make pEPSA\_ylaN was used to make pCM28\_ylaN. The forward primer and reverse primer are pcm28ylaNforYC and pcm28ylaNrevYC, respectively. Together these primers form a PCR product from 138bp upstream of *ylaN*, which includes the native promoter, to 57bp from the end of *ylaN*. The plasmid template was provided by strain JMB4809. Digestion enzymes used were BamHI and MluI.

**Chromosomal deletion of *ylaN*:** The region directly upstream of *ylaN* (-615 to -1) was amplified using primer pair YCCyalaNupFor and ylaNuptetRev. The downstream region, 26pb past *ylaN* plus an additional 678bp, was amplified using primer pair tetRylaNdwnfor and ylaNdwnpJB38. A tetracycline cassette was amplified from strain JMB7382 using primers ylaNuptetRfor and tetRylaNdwnrev, which contain complementary DNA to primers ylaNuptetRev and tetRylaNdwnfor, respectively. YCCyalaNupFor and ylaNdwnpJB38 both contain complementary DNA with plasmid pJB38\_YCC. pJB38\_YCC was isolated from an overnight culture of strain JMB7382, digested with SalI and NheI, and purified by gel extraction. The three PCR products and the digested plasmid were combined by homologous recombination in yeast, forming the chromosomal insertion vector pJB38\_Δ*ylaN*::*tet*. The vector was transformed into RN4220 and incubated at 30°C. Chromosomal insertion was achieved through selection by temperature (37°C) and kanamycin (Bose et al., 2013). Colonies were scored for tetracycline and kanamycin resistance.

**Multicopy Complementation Mutant pEPSA\_ylaN<sub>C38A</sub>:** A C38A amino acid change was made on YlaN using site-directed mutagenesis. Primer pairs pEPyalaNforYC and ylaNC38Arev, and pEPyalaNrevYC and ylaNC38Afor, were used to amplify overlapping sections of *ylaN* while inducing the mutations 112T>G and 113G>C. The PCR products and digested and purified pEPSA plasmid were combined into a vector by the yeast cloning methods mentioned above.

#### Plate Spotting Assays

Cells were grown overnight in TSB until the late stationary phase (~18 h). 300 µL from each culture was transferred to a sterile 1.5 mL centrifuge tube and pelleted by centrifugation.

The pellets were washed twice and then resuspended in sterile 1 mL Phosphate Buffered Solution (PBS), pH 7.4. A serial 1:10 dilution was performed on each strain to a total dilution factor of  $10^6$ . Four  $\mu$ L of each sample was pipetted onto appropriate plates and incubated overnight at 37°C. Plates included in this research: TSA, TSA with chloramphenicol, TSA + 700  $\mu$ M 2,2-dipyridyl (DIP), TSA + 20 mM Methyl Viologen. Induction of pEPSA occurred by the addition of xylose to the media.

#### Growth Curve Assay using Plate Reader

Cells were grown overnight in TSB until the late stationary phase (~18h). 800  $\mu$ L of the culture was transferred into a sterile 1.5 mL microcentrifuge tube and cells were pelleted by centrifugation. The cells were washed twice with 1 mL sterile PBS and then resuspended in 1 mL PBS. The OD was measured using a Beckman Coulter DU530 UV-vis absorption spectrophotometer ( $\lambda=600$  nm). Cultures were diluted to an OD of 0.2 in PBS. Two  $\mu$ L of each sample was added to wells containing 198  $\mu$ L of 0.5X TBS with trace metals solution, with and without 100  $\mu$ M FeSO<sub>4</sub>. PBS was added to any empty well to prevent evaporation during the experiment. The plate was covered with the lid and sealed with Parafilm and incubated at 37°C with shaking in a BioTek El808 spectrophotometer. The absorbance at  $\lambda=630$  nm was read at 30 minutes intervals for 13 hours. The final concentration of trace metals solution can be found in **Table 4**.

#### Aconitase Assays

The aconitase assay was performed according to previously described methods (Mashruwala et al., 2015) with slight modifications. One mL of growth media was inoculated

with 10  $\mu$ L from cultures grown overnight. These were grown to late stationary phase (~18 h) at 37°C with shaking. 800  $\mu$ L of each sample was transferred to a 1.5 mL microcentrifuge tube, and cell pellets were formed by centrifugation. The supernatant was removed, and the remaining pellets were stored at -80 °C for at least 4 hours. The cell pellets were thawed in an anaerobic chamber for 10 minutes and then resuspended in 100  $\mu$ L of anaerobic lysis buffer (100 mM Tris-HCl, 150 mM NaCl pH 7.4, 200  $\mu$ M DNase, 200  $\mu$ M Lysostaphin) and incubated at 37 °C for 1 hour until the lysate cleared. Pellets were formed by centrifugation at 3000 rpm anaerobically for 10 minutes. 90  $\mu$ L of the cell-free lysate was transferred to new centrifuge tubes and closed before removal from the anaerobic chamber. 10  $\mu$ L of the cell-free lysate was added to 970  $\mu$ L of buffer (100 mM Tris-HCl, 150 mM NaCl pH 7.4) and 20  $\mu$ L of 2 mM DL-isocitrate. The conversion of isocitrate to cis-aconitase was measured using a Beckman Coulter DU530 UV-vis absorption spectrophotometer (cis-aconitase  $\epsilon_{240 \text{ nm}} = 3.6 \text{ mM}^{-1} \text{ cm}^{-1}$ ). The protein concentration was determined using the BCA method with a BSA standard. The specific activity was determined as the moles of product formed/minutes/protein (Kennedy et al., 1983). For the assay measuring chromosomal *acnA* activity of the wildtype (WT) and  $\Delta ylaN$ , TSB was used as the growth medium. TSB with 0.001% CM and 120  $\mu$ M DIP was used to measure the effects of iron limitation on  $\Delta acnA \text{ } pancA$  and  $\Delta acnA \Delta ylaN \text{ } pancA$ .

#### H<sub>2</sub>O<sub>2</sub> Killing Assay

Cells were grown overnight in TSB until the late stationary phase (~18 h). 800  $\mu$ L of the culture was transferred into a sterile 1.5 mL microcentrifuge tube and pelleted by centrifugation. The pellets were washed twice with 1 mL sterile PBS and then resuspended in 1 mL PBS. The OD was found using a Beckman Coulter DU530 UV-vis absorption spectrophotometer ( $\lambda=600 \text{ nm}$ ) and standardized to a volume of 1 mL with an OD of 0.7 in PBS. H<sub>2</sub>O<sub>2</sub> was added to the cells to a concentration of 1.5 M and incubated for two hours at room temperature. 50  $\mu$ L of each

reaction mixture was diluted 1:20 with PBS containing catalase (~1300 units/mL) in sterile 2 mL microcentrifuge tubes and incubated for five minutes. 1:10 serial dilutions were performed and spotted on TSA plates and incubated overnight at 37 °C.

### Streptonigrin Assay

The assay was performed according to previously described methods (Mashruwala et al., 2016) with slight modifications. Cells were grown overnight in TSB until the late stationary phase (~18 h). The cultures were diluted to an OD of 0.1 in TSB. 100 µL of the diluted culture was added to 4 mL of soft TSA (3.5% agar) and vortexed briefly, overlaid on TSA plates containing chloramphenicol, and left to rest at room temperature for 20 minutes. 5 µL of streptonigrin (2 mg/mL in DMSO) was added to the center of the plate. Plates were incubated overnight at 37 °C and the area of inhibition measured.

### Protein Expression and Purification

*E. coli* containing pGEX\_ylaN (strain JMB8478) was grown overnight to stationary phase in LB media containing ampicillin, and the plasmids harvested using a plasmid isolation kit. Isolated plasmids were transformed by electroporation into BI21 *E. coli* (strain JMB437) and plated on LB containing ampicillin. A 50 mL overnight culture was started from an amp resistant colony. The following morning, two 2 L flasks containing LB-ampicillin were inoculated to an OD of 0.5. The cultures were grown with shaking at 37 °C to an OD of 1. Cells were induced using 1 mM IPTG and 0.1% w/v arabinose and grown at 30 °C for 4 hours. The cells were harvested by centrifugation (~7000 rpm for 15 minutes) and stored overnight in a -80 °C freezer. The cell pellets were thawed and resuspended in PBS to a total volume of 35 mL. DNAase was added to the sample and vortexed. The cells were lysed using a French press, and the cell debris was pelleted by centrifugation (~15,000 rpm for 30 minutes). The protein was purified using the



GE Healthcare GST trap system and salt column chromatography according to the manufacturer's instructions. The purified protein was verified using SDS-PAGE gel electrophoresis.

#### Competitive competition via 1,10-phenanthroline

Methods were followed according to McKenzie et al. (2016). Briefly, different concentrations of purified YlaN were added to fixed concentrations of 1,10-phenanthroline and  $\text{Fe}^{2+}$ . The concentration of the 1,10-phenanthroline and  $\text{Fe}^{2+}$  complex was measured using a BioTek EL808 spectrophotometer at a wavelength of 510 nm.

#### Competitive competition via MagFura-2

Methods were followed in accordance with Rodriguez et al. (2015) with minor changes. MagFura-2 binds divalent transition metals. The apo form of MagFura-2 has a maximum absorption peak at 366 nm, while the metal-bound form shows a peak at 325 nm. MagFura-2 was added to buffer (50 mM Tris-HCl, 150 mM NaCl, 15% glycerol, pH 7.8) in a concentration between 2 to 4  $\mu\text{M}$ . Aliquots of 2 mM  $\text{Fe}^{2+}$  were added to the MagFura-2 in the presence and absence of purified YlaN (4.9  $\mu\text{M}$ ), and the absorption spectra were measured between 450 and 250 nm. To correct for background absorption, the same volumes of  $\text{Fe}^{2+}$  were added to buffer only, and the absorbance spectra were subtracted from the spectra of MagFura-2 only and MagFura-2 plus YlaN. The total starting volumes, with and without protein, were equal to 1 mL. The assay was performed anaerobically. YlaN was reduced with 5 mM Tris(2-carboxyethyl)phosphine hydrochloride (TCEP) before its addition to MagFura-2. A 1 cm quartz cuvette was used. Initial concentrations of MagFura-2 and YlaN were found using their molar absorption in the iron-free buffer,  $\epsilon=29,900 \text{ M}^{-1} \text{ cm}^{-1}$  at 366 nm, and  $\epsilon=1,490 \text{ M}^{-1} \text{ cm}^{-1}$  at 280 nm, respectively.

Sequence alignments, protein visualization, and gene tree construction

DNA and amino acid sequence data for SAUSA300 *ylaN* was retrieved from the KEGG database (Kanehisa et al., 2002). A Blast search was performed with the amino acid sequence to identify homologous proteins. Sequences from organisms within the same genus and from different genera were chosen for alignment to determine conserved amino acid residues. E values ranged from 1e-57 to 2e-8. Twenty-nine sequences were aligned in MEGA7 (Kumar et al., 2016) using ClustalW, with standard parameters. The maximum likelihood method was used to estimate the phylogenetic history of YlaN using the amino acid sequences, with the JTT matrix model used for amino acid substitutions over time (Jones et al., 1992). Gaps and missing data were not used in the analysis, leaving 86 positions for the analysis. Protein visualization was performed using Dassault Systèmes Biovia, Discovery Studio Visualizer, 2017R2 (Dassault Systèmes, 2017). The protein structure of YlaN was downloaded from the Protein Data Base, ID: 20DM (Xu et al., 2007).

## Results

### Construction of a *ylaN* mutant in *Staphylococcus aureus*.

A *ylaN* deletion was created in the *Staphylococcus aureus* strain SAUSA300. A tetracycline marker was used to replace chromosomal *ylaN*. The marker was cloned onto a chromosomal insertion plasmid by yeast cloning and transformed into *S. aureus*. Chromosomal insertion was selected for using temperature sensitivity and selection by kanamycin. Insertion was verified using PCR. These data verified that YlaN is not essential for *S. aureus*. The  $\Delta$ *ylaN* strain did not display growth abnormalities when cultured on complex or defined media (data not shown).

### **A *ylaN* mutant displays reduced growth in the presence of 2,2'-dipyridyl.**

2,2'-dipyridyl (DIP) is a cell-permeable chelating agent that binds to divalent metals such as  $\text{Fe}^{2+}$ . Bacteria lacking the genes needed to mature FeS clusters often have reduced growth in the presence of DIP (Outten et al., 2004). The growth of  $\Delta ylaN$  on solid complex media was similar to WT (**Figure 1, Panel A**). The  $\Delta ylaN$  strain grown in DIP treated media showed a 3-log reduction in growth when compared to WT (**Figure 1, Panel B**). Returning the *ylaN* gene to the  $\Delta ylaN$  strain, via complementation plasmid, corrected the growth defect confirming that the lack of YlaN was leading to the phenotype noted.

### **A *ylaN* mutant shows reduced growth in liquid medium lacking Fe.**

YlaN is essential in *B. subtilis* when cultured under typical laboratory growth conditions; however, it is non-essential when excess iron is added to the media (Peters et al., 2017). We found that the *S. aureus*  $\Delta ylaN$  strain had decreased growth when cultured in the presence of DIP, which can associate with a variety of metals. We tested the hypothesis that YlaN is required for *S. aureus* growth under Fe limiting conditions. Chelex-100 is a compound that binds transition metals (Koshima, 1986). 0.5xTSB was treated with Chelex-100 and then filtered to remove the Chelex-100 and the associated metals. Trace metals, excluding iron, were added back to the media. The  $\Delta ylaN$  strain had reduced growth when compared to the WT strain when grown in the treated media lacking iron (**Figure 2, Panel A**). The addition of Fe improved the growth of the  $\Delta ylaN$  strain (**Figure 2, Panel B**).

**Aconitase activity was decreased in a  $\Delta ylaN$  strain, and the phenotype was exacerbated when Fe is limiting.**

Aconitase (AcnA) is an FeS cluster requiring enzyme (Kennedy et al., 1983) that catalyzes the interconversion of citrate and isocitrate. *S. aureus* strains lacking genes needed to build and transport FeS clusters show reduced aconitase activity (Marshuwala et al., 2016). The WT and  $\Delta ylaN$  strains were grown to late stationary phase, and aconitase activity was quantified in cell-free lysates. The  $\Delta ylaN$  strain displayed over 20% decrease in AcnA activity when compared to the wild-type (**Figure 3, Panel A**).

To genetically complement the  $\Delta ylaN$  strain, *ylaN* was added back on a plasmid under the transcriptional control of a xylose inducible promoter. When not induced,  $\Delta ylaN$  pEPSA\_ylaN showed over 20% decrease in AcnA activity (**Figure 4**), similar to what was seen previously (**Figure 3, Panel A**). Upon induction with 2% xylose, AcnA activity of  $\Delta ylaN$  pEPSA\_ylaN surpassed that of the WT strain with the empty vector (pEPSA) (**Figure 4**).

Aconitase transcription is greatly repressed upon Fe limitation; therefore, we could not add DIP to the cells to mimic Fe limitation. To overcome this obstacle, we used strains that have *acnA* under the transcriptional control of a xylose inducible promoter. We monitored AcnA activity in the  $\Delta acnA$  and  $\Delta acnA \Delta ylaN$  mutants containing pEPSA\_acynA after culture in the presence and absence of 120  $\mu$ M DIP. AcnA activity was greatly decreased in the  $\Delta acnA \Delta ylaN$  strain when cultured in the presence of DIP suggesting that YlaN has a role in maturing AcnA under Fe limiting conditions (**Figure 3, Panel B**).

#### **A $\Delta ylaN$ strain has increased resistance to streptonigrin.**

Streptonigrin in complex with Fe and an electron donor can catalyze DNA lesions resulting in cell death. The more cytoplasmic free (also called non-chelated) Fe a cell has the more sensitive it is to streptonigrin (Yeowell and White, 1983). The data presented so far suggest that strains lacking YlaN have defective growth when Fe is limiting. One interpretation of these

data is that a  $\Delta ylaN$  strain has less cytosolic Fe that could be used to metalate proteins. We tested the hypothesis that a  $\Delta ylaN$  strain has less streptonigrin accessible Fe and increased resistance to streptonigrin. We created top agar overlays containing either the WT or the  $\Delta ylaN$  mutant and spotted streptonigrin atop the overlay. The  $\Delta ylaN$  strain was less sensitive to killing by streptonigrin than the WT strain, and the phenotype could be genetically complemented (**Figure 5**).

### **A $\Delta ylaN$ strain has increased resistance to killing by $H_2O_2$**

$H_2O_2$  can react with free iron inside the cell to produce hydroxyl radicals, which can ultimately result in cell death. Therefore, Fe and FeS containing proteins and FeS assembly proteins which bind iron are important in limiting the amount of free iron within the cell (Keyer and Imlay, 1996). We treated cultures of WT and  $\Delta ylaN$  strains with 1.5 M  $H_2O_2$  and subsequently spot plated the strains on TSA plates to determine if  $\Delta ylaN$  would also decrease survival when challenged with  $H_2O_2$ . Both the WT and  $\Delta ylaN$  strains were killed by  $H_2O_2$ ; however, the  $\Delta ylaN$  strain had one log more growth than the WT strain, meaning it is less sensitive to damage by  $H_2O_2$  (**Figure 6**). A catalase (*kat*) mutant was included as a positive control.

### **The $\Delta ylaN$ strain has decreased survival when challenged with methyl viologen, and over-expression of *ylaN* exacerbates the phenotype.**

Methyl viologen is a redox cycling compound that catalyzes ROS production. It also produces superoxide ions inside the cell (Bus and Gibson, 1984). *S. aureus* strains lacking *sufBCDSU* genes show sensitivity to methyl viologen. We spotted strains lacking *ylaN* on TSB

containing methyl viologen to see if it would phenocopy *sufBCDSU* strains. The *ΔylaN* strain with pEPSA showed a three log reduced growth when compared to the WT with pEPSA (**Figure 7**). Interestingly, the *ΔylaN* containing pEPSA\_*ylaN* did not complement but caused a reduction in survival. A two-log decrease in growth was seen in *ΔylaN* with pEPSA\_*ylaN* when compared to *ΔylaN* with pEPSA in both the induced and un-induced media. A further reduction in growth by two logs also occurred in the *ΔylaN* mutant with pEPSA\_*ylaN* upon induction of transcription.

### **The strictly conserved cysteine 38 of YlaN is not necessary for the aconitase activity and methyl viologen phenotypes.**

The amino acid cysteine contains a thiol group which can act as a nucleophile and donate electrons and participate in redox reactions. Cysteine can also function in Fe and Fe-S cluster binding. Our initial sequence alignment showed one conserved cysteine at amino acid position 38 (**Figure 8, Panel C**). By examining the crystal structure of YlaN we found that the cysteine is cytosolic (**Figure 9**) when YlaN is in its dimer form. We substituted the cysteine with alanine using site-directed mutagenesis. We introduced this allele into the *ylaN* mutant to investigate the effects of this substitution (pEPSA\_*ylaN*<sub>C38A</sub>). The mutated pEPSA\_*ylaN*<sub>C38A</sub> allele complemented both the aconitase phenotype (**Figure 4**) and the methyl viologen phenotype (**Figure 7**) to a degree that was similar to complementation with the wild-type allele. This indicates that the conserved cysteine does not play a role in the *in vivo* iron-dependent phenotypes we have observed. The altered nucleotide sequence of the strain transformed with pEPSA\_*ylaN*<sub>C38A</sub> was confirmed by DNA sequencing (**Figure 8, Panel A and B**).

### **Eleven conserved amino acid residues were identified among YlaN homologs.**

The amino acid alignment of the 29 YlaN homologs revealed 11 conserved amino acid residues: Ilu22, Ilu26, Cys38, Asp46, Thr47, Gln48, Gly51, Ala59, Gly70, Leu77, and Glu78 (**Figure 8, Panel C**). Residue Cys38 is located on a solvent exposed section of YlaN when it is in dimer formation (**Figure 9**).

### **The presence of protein domains DUF1507 and DUF2680 is not monophyletic.**

YlaN in *S. aureus* contains two domains of unknown function, DUF1507 and DUF2680, as identified by the KEGG database and GenomeNet (**Figure 10**). The DUF1507 has an iEvalue of  $1.7e-36$  while the DUF2680 domain has an iEvalue of 0.0027. The presence of both motifs on YlaN homologs is not monophyletic within the *Staphylococcus* genus (**Figure 11**). *S. saprophyticus* and *S. equorum* do not contain the DUF2680 domain. Half of the YlaN homologs from outside the genus *Staphylococcus* do not contain the DUF2680 domain.

### **Purified YlaN prevents 1,10-phenanthroline from binding iron.**

Recombinant YlaN was expressed and purified from *Escherichia coli*, strain BL21, cells. YlaN purity was determined to be >95% pure by SDS-PAGE gel electrophoresis (**Figure 12, Panel A**). 1,10-phenanthroline absorbs visible light when bound to  $Fe^{2+}$ . We tested the hypothesis that YlaN could outcompete 1,10-phenanthroline for  $Fe^{2+}$  binding. Different concentrations of YlaN were combined with fixed concentrations of 1,10-phenanthroline and  $Fe^{2+}$ . The concentration of the 1,10-phenanthroline and  $Fe^{2+}$  complex was monitored using visible absorption spectroscopy. As the concentration of YlaN was increased the concentration of the

$\text{Fe}^{2+}$ :1,10-phenanthroline complex decreased (**Figure 12, Panel B**) suggesting that YlaN is competing with 1,10-phenanthroline for  $\text{Fe}^{2+}$  or preventing binding.

### **Examining of YlaN $\text{Fe}^{2+}$ binding properties using MagFura-2.**

A competition assay was performed anaerobically to determine the iron-binding properties of YlaN using a compound with known iron-binding properties. MagFura-2 is a compound that binds to  $\text{Fe}^{2+}$  in a 1:1 ratio (Rodrigues, 2015; Patel et al., 2016). In its apo-state, MagFura-2 shows peak absorption at 366 nm, and this peak decreases upon  $\text{Fe}^{2+}$  binding. Its metal-bound holo-form has a peak that increases at 325 nm. The absorbance at 366 nm decreased for MagFura-2 both in the presence and absence of YlaN as an increasing concentration of  $\text{Fe}^{2+}$  was added (**Figure 13, Panel A and B**). The insets in each graph show the MagFura-2 spectral changes between 250 nm and 450 nm with the addition of  $\text{Fe}^{2+}$ . In both graphs, the arrows show that the absorbance peak at 366 nm decreases with the addition of  $\text{Fe}^{2+}$  while the peak at 325 nm increases, meaning the concentration of apo MagFura-2 decreases with the addition of iron. When normalized to absorbance per 1  $\mu\text{M}$  MagFura-2, the data shows that MagFura-2 binds iron in a higher amount in the presence of YlaN (**Figure 13, Panel C**).

## **Discussion**

The ability to build FeS clusters is essential in *Staphylococcus aureus*. When cells are unable to synthesize FeS clusters, vital metabolic processes shut down, which eventually results in cell death (Valentino et al., 2014; Mashruwala et al., 2015; Mashruwala et al., 2016). In this study, we investigated the role of YlaN in FeS cluster generation and Fe homeostasis. We tested the hypothesis that *S. aureus* strains lacking *ylaN* would have similar phenotypes to strains



lacking genes which are known to be involved in FeS formation, namely *sufBCDSU*. We looked at the iron binding ability of purified YlaN and tried to determine the amino acid needed for aconitase activity and resistance to methyl viologen. Understanding how FeS clusters are formed inside the cell is important. *S. aureus* lacking genes needed for FeS synthesis were found to have reduced fitness in mouse models of infection; however, they were more persistent and resistance against certain antibiotics (Mashruwala et al., 2015). Lastly, the mechanisms by which *S. aureus* builds FeS clusters is different from that of mammals suggesting that FeS cluster synthesis and the maturation of FeS proteins is an antimicrobial target.

We found that strains lacking YlaN have a similar phenotype to strains lacking SufBCDSU. The *ylaN* mutant showed reduced growth when iron availability was limited due to 2,2'-dipyridyl or when the media was treated with Chelex-100 to remove Fe. The phenotypes were partially corrected either by plasmid complementation or by addition of iron to the media. These results show that *ylaN* has a role in iron homeostasis in *S. aureus*. Similarly, in *B. subtilis*, YlaN is essential under normal laboratory growth conditions. *B. subtilis* strains lacking YlaN do not grow on LB media; however, this can be corrected with the addition of  $\text{Fe}^{3+}$  (Peters et al., 2017). Additionally, we found that strains lacking YlaN were resistant to streptonigrin, an antibiotic which causes cell death in the presence of iron (Cohen et al., 1987). An increase in intracellular iron has been shown to increase sensitivity to streptonigrin (Yeowell and White, 1983). The work of Peters et al. (2017) and our own data suggest that *ylaN* plays a role in iron availability inside the cell.

*S. aureus* strains lacking genes needed for FeS cluster synthesis show reduced aconitase activity (Mashruwala et al., 2015; Rosario-Cruz et al, 2015; Mashruwala et al., 2016). The *ylaN* mutant showed a reduction in aconitase activity over 20%. The reduction in activity could be attributed to several factors: failure to maturate and insert the  $[\text{Fe}_4\text{S}_4]$  cluster needed for the enzyme to function, ROS damage to the FeS cluster resulting in the inactive  $[\text{Fe}_3\text{S}_4]^{+1}$  state, or

reduced expression of the AcnA enzyme. When an *acnA ylaN* strain with *pacnA* was grown in the TSB with 120  $\mu$ M DIP, the aconitase activity of  $\Delta ylaN$  decreased by 40% when compared to its growth in TSB only, while the activity of the *acnA::tn* with *pacnA* increased. This data shows that YlaN is important for the maturation of FeS clusters when cells are under stress due to low iron conditions.

FeS clusters and FeS cluster containing proteins are oxidation targets for ROS. *S. aureus* strains lacking proteins needed for FeS cluster maturation have decreased resistance to compounds which induce ROS formation, including H<sub>2</sub>O<sub>2</sub>. Surprisingly,  $\Delta ylaN$  showed a small resistance to killing by H<sub>2</sub>O<sub>2</sub> when compared to the WT strain. Lack of free Fe in the cell could result in less killing by H<sub>2</sub>O<sub>2</sub>.

$\Delta ylaN$  showed an interesting phenotype when exposed to methyl viologen. While  $\Delta ylaN$  showed reduced growth in the presence of methyl viologen, similar to other strains lacking FeS assembly genes, complementation with a functioning *ylaN* gene results in increased cell death. A possible explanation for these results is that YlaN is involved in iron regulation, possibly by binding to Fur and inhibiting its binding to Fe. Apo-Fur upregulates genes needed in Fe acquisition. Therefore, a strain lacking YlaN would have low expression of iron acquisition genes, low intercellular Fe, and low free Fe, because YlaN is not there to prevent holo-Fur from forming. Superoxide dismutase (SodA) is an enzyme that helps protect the cell from damage due to superoxide radicals by breaking superoxide down into H<sub>2</sub>O<sub>2</sub> and O<sub>2</sub>. In *E. coli*, the expression of *sodA* is regulated by Fur and the Arc (aerobic respiration control) protein (Tardat et al., 1991) and it is downregulated under high Fe conditions by holo-Fur (Niederhoffer et al., 1990). If *sodA* in *S. aureus* is similarly controlled, then strains lacking YlaN would have less protection against superoxide radicals formed by the methyl viologen treatment. Over expression of *ylaN* would form apo-Fur complexes which would bring more iron into the cell. An increase in free cellular iron in the presence of ROS generated by methyl viologen could also lead to reduced growth due

to hydroxyl radicals produced by Fenton and Haber-Weiss reactions. Based on the results of this experiment, possible interactions of YlaN with Fur should be investigated.

YlaN was found to inhibit 1,10-phenanthroline from complexing with Fe, but it did not inhibit the binding of  $\text{Fe}^{2+}$  to MagFura-2. The  $K_d$  of MagFura-2:: $\text{Fe}^{2+}$  complex was experimentally determined to be  $2.05\mu\text{M}$  (+/- 0.07) (Rodrigues, et al., 2016) and the  $K_d$  for 1,10-phenanthroline:: $\text{Fe}^{2+}$  is  $1.3\mu\text{M}$  (Lee et al., 1948), meaning that if *ylaN* is able to bind  $\text{Fe}^{2+}$  in the presence of 1,10-phenanthroline, then it should also be able to bind it in the presence of MagFura-2. The competition assay with MagFura-2 was performed anaerobically, while the assay with 1,10-phenanthroline was performed aerobically.  $\text{Fe}^{2+}$  can easily be oxidized to  $\text{Fe}^{3+}$  in the presence of  $\text{O}_2$ ; therefore, YlaN might bind  $\text{Fe}^{3+}$  instead of  $\text{Fe}^{2+}$ . This would still reduce the amount of  $\text{Fe}^{2+}$  available for 1,10-phenanthroline binding and explain our results. The 1,10-phenanthroline assay should be performed again in an anaerobic setting. No reduction in absorbance with the addition of YlaN inside an anaerobic chamber would indicate the lack of YlaN binding to  $\text{Fe}^{2+}$ , or to  $\text{Fe}^{3+}$  that was produced by oxidation. The binding of YlaN to  $\text{Fe}^{3+}$  would then need to be investigated.

The *ylaN*<sub>C38A</sub> allele complemented some of the phenotypes of the  $\Delta$ *ylaN* strain indicating that this residue is not necessary for the phenotypes examined. Further investigation revealed that during the initial characterization of purified YlaN, the electron density map showed an unknown ligand bound to a pocket within each half of the dimer bracketed by conserved residues Ile22 and Gly51. The pocket was further surrounded by semi-conserved amino acids, Asp18, Ala19, Gln48, Leu52, and Glu55. (Xu et al., 2007). Of these 5 amino acids, only Gln48 matches the conserved residues we found within our sequence alignment. Gln48 is the only polar residue of the three conserved amino acids, making it the candidate for the next round of site-directed mutagenesis.

The conserved amino acids list I created is made from protein sequences identified as YlaN homologs by KEGG. It is important to note, though, that not all the sequences contain both protein domains DUF1507 and DUF2680 like the *S. aureus* sequence. Within the genus *Staphylococcus*, *S. saprophyticus* and *S. equorum* do not contain DUF2680. Half of the sequences from outside of the genus *Staphylococcus* do not contain the DUF2680 motif. As this was just a preliminary investigation of where YlaN can be found within the bacterial kingdom, a more in depth phylogenetic and bioinformatic analysis should be undertaken. Separate alignments of each domain should be performed. Conserved sites within the DUF2680 domain may be revealed when individuals missing the domain are removed. Comparison of the presence or absence of DUF2680 in YlaN with genes needed in FeS cluster maturation, iron homeostasis, and pathways using FeS proteins might also help identify the purpose of YlaN within different species. GenomeNet identified the DUF2680 domain as belonging to the family of proteins within *B. subtilis* known as yckD. It is also important to note that the iEvalue of DUF2680 is very low, meaning the sequence varies greatly from the Pfam ID sequence used for identification. Moving forward, we should be open to the possibility that YlaN has different functions within different organisms, due to the presence of different protein motifs.

The next steps of this project include investigating the Fe<sup>3+</sup> binding capability of YlaN and further investigating the role YlaN has on free iron in the cell, as indicated by the streptonigrin assay. Increased free iron in the cell can lead to high rates of mutation, due to ROS damage of DNA. Therefore, we could compare the mutation rates of *ΔylaN* and WT strains. Higher mutation rates in the WT strain would support the lack of free iron in strains missing *ylaN*. We could also quantify the total amount of free iron in the cell using cell lysate and a colorimetric analysis, similar to the 1,10-phenanthroline assay. We could also quantify total cellular Fe using ICPMS to determine if there is a difference in total Fe load.

If *ylaN* is shown to alter the free iron available in the cell, then the mechanism of how it does this should be investigated. Transcriptional reporter assays involving the Fur promotor attached to GFP could be an easy first look into the effects of *ylaN* on iron regulation within the cell. Then transcription analysis of iron-uptake genes in the Fur regulon in WT and *ylaN* mutants could be compared using qPCR.

In conclusion, our data supports a role for YlaN in iron homeostasis within the cell, which makes it important in the maturation of FeS clusters in *S. aureus* under low iron conditions. Initial results also show that YlaN inhibits the binding of 1,10-phenanthroline to free Fe. This research has provided an initial framework with which to investigate the function of YlaN in *S. aureus*.

**Table 1: Primers Used in this Research**

Name	Sequence
ylaNC38Arev	CTTCTTCATATAATGGGGCTGAAGGTAATGTTAAA
ylaNC38Afor	TTTAACATTACCTTCAGCCCCATTATGAAGAAG
pcm28ylaNforYC	GTAATATAGCGTAACTATAACGGTCCTAACGCGTCCCACTCCCTATCAATGTATATA
pcm28ylaNrevYC	GATTACGAATCCATGATCGAATGCTAGCGGATCCGGCGCAGCTCAATTGTCGATATC
ylaNdwnpJB38	TGAAATCAGAGCTTGCATGCCTGCAGGTCGACCCGTGAAGTTCATAAAATCCTAAGTTT
tetRylaNdwnfor	GTATATAAACATTCTCAAAGGGATTTCTAAACGCGTGGCGTGAGATATCGACAATTG
ylaNuptetRfor	ATTTATATAGAGGGGAGCGTGTACGCGTCGGATTTTATGACCGATGATGAAGAAA
tetRylaNdwnrev	CTCAATTGTCGATATCTCAGCCACGCGTTTAGAAATCCCTTTGAGAATGTTTATATA
YCCylaNupfor	ATAGCGTAACTATAACGGTCCTAATGTGCGCTAGCCCTCAATATGAGTTACATGGTT
ylaAuptetRrev	CTTTTCTTCATCATCGGTCATAAAATCCGACGCGTGACACGCTCCCCCTCTATATAA
pEPylaNrevYC	GCGTAACTTTTCCCCGAAAAGTGCCACCACGCGTGCTCAATTGTCGATATCTCACGC
pEPylaNforYC	CGAGCTCGGTACCCGGGGATCCTCTAGAGTCGACGAGGGGGAGCGTGTCATGGCGA
ylaNGSTBamHI	GGGGGATCCATGGCGAAACAAGCAACAATGAAAAATGCAG
ylaN3XhoI	GGGCTCGAGTTAAACAAGTGTAAGGCTTCATGTAATTTTG
acnA3saI	CCCGTCCACGAGCACTATCAAAGTGC
acnApHindIII	GGGAAGCTTCTGACATTCTTGAAAAG

**Table 2: Strains Used in this Research**

JMBStrain	Genotype
1100	WT USASA300
1103	RN4220 (electrocompetent cells)
1402	pCM28
1304	pEPSA
8697	$\Delta ylaN$ pEPSA
8698	$\Delta ylaN$ pEPSA_ylaN
9198	$\Delta ylaN$ pEPSA_ylaN_C $\rightarrow$ A
1242	pCM28
8695	$\Delta ylaN$ pCM28
8696	$\Delta ylaN$ pCM28_ylaN
8428	ylaN:: <i>erm</i>
2078	katA:: <i>erm</i>
8689	$\Delta ylaN$ :: <i>tet</i>
3537	AncA:: <i>erm</i> pEPSA_AcnA_Flag
8706	AncA:: <i>erm</i> $\Delta ylaN$ pEPSA_AcnA_Flag
1176	pCM28 <i>E. coli</i>
1177	pEPSAS <i>E. coli</i>
1600	pJB38 <i>E. coli</i>
7588	pGEX_GP1 <i>E. coli</i>
1627	BL21 AI* <i>E. coli</i>
7751	pEPSA template with YCC cassette
4809	pCM28 template with YCC cassette
7382	pJB38 template with YCC cassette

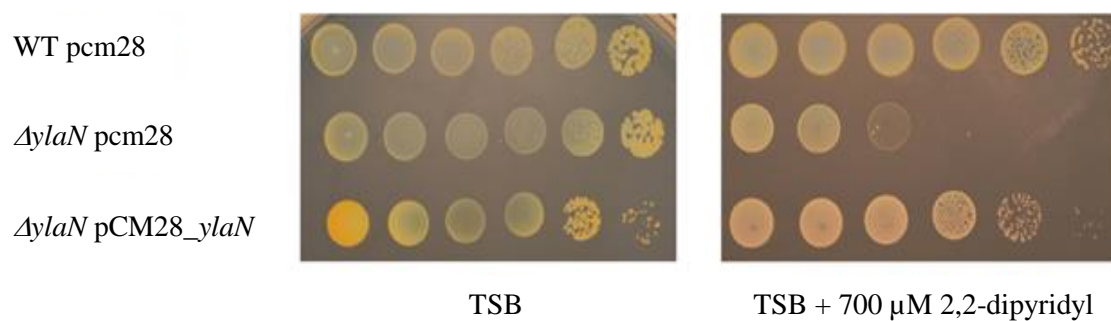
**Table 3: Plasmids Used for Strain Construction**

Name	Purpose	Source
pEPSA	Multicopy complementation with an inducible promoter	Forsyth et al., 2002
pCM28	Complementation using a native promoter	Pang et al., 2010
pJB38	Chromosomal insertion	Bose et al., 2013
pGEX	Expression and protein purification	GE Healthcare

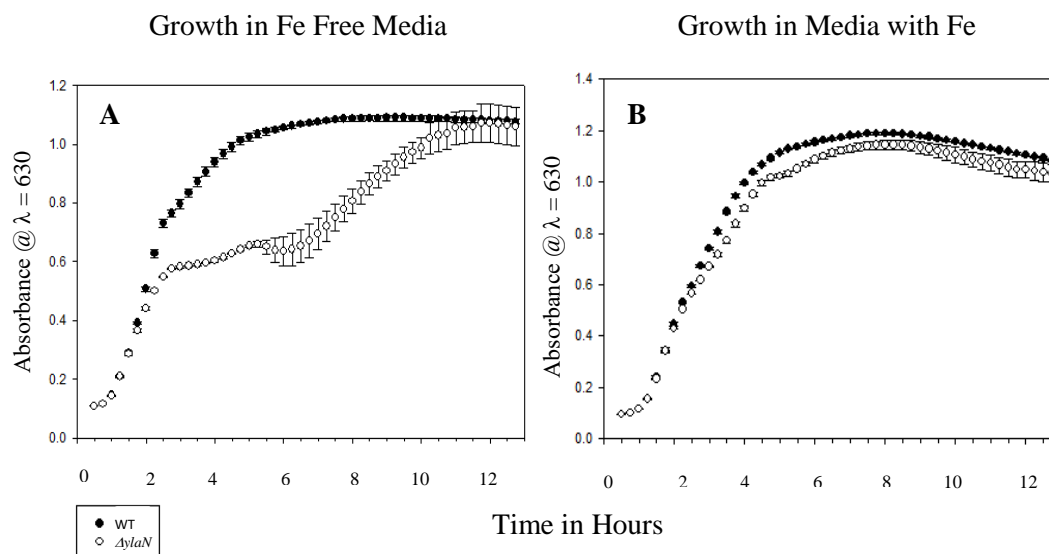
**Table 4: Trace Minerals Solution**

Mineral	Final Concentration $\mu\text{M}$
Nitrilotriacetic acid	530
MnSO <sub>4</sub> 4H <sub>2</sub> O	90
NaCl	171
CoSO <sub>4</sub>	800
CaCl <sub>2</sub> 2H <sub>2</sub> O	70
ZnSO <sub>4</sub>	60
CuSO <sub>4</sub> 5H <sub>2</sub> O	4
H <sub>3</sub> BO <sub>3</sub>	20
Na <sub>2</sub> MoO <sub>4</sub> 2H <sub>2</sub> O	120
Na <sub>2</sub> SeO <sub>4</sub> 10H <sub>2</sub> O	110
NiSO <sub>4</sub> 6H <sub>2</sub> O	20





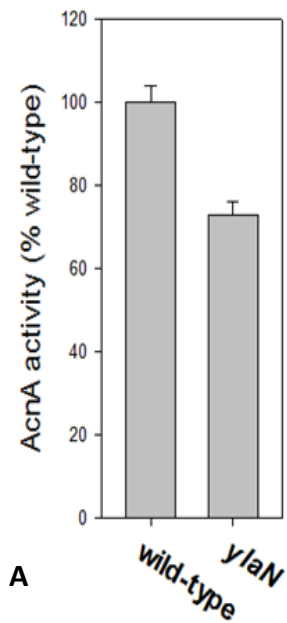
**Figure 1: Growth in the presence and absence of 2,2-dipyridyl.** Overnight cultures of the WT with pCM28 (empty vector) and the  $\Delta ylaN$  mutant with either pCM28 or pCM28\_ylaN were serial diluted and spot plated on TSB medium with and without 700 μM 2,2-dipyridyl. A representative picture is shown.



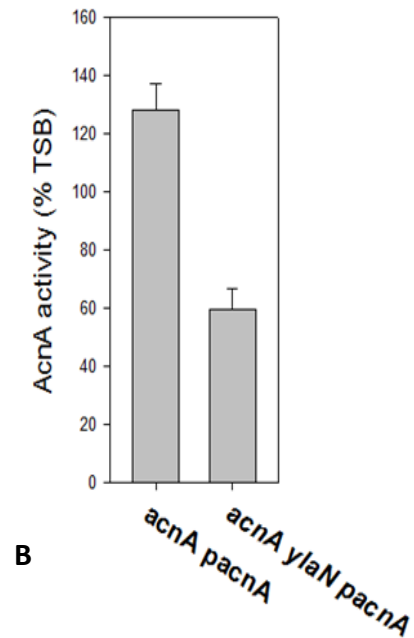
**Figure 2: Growth in Fe deplete media with and without supplemented Fe.**

Panel A. The growth of WT and  $\Delta ylaN$  strains in TSB medium that had been treated with Chelex-100 to remove divalent trace metals and supplemented with a trace metal mixture lacking Fe are shown. Panel B. Growth of the WT and  $\Delta ylaN$  strains in the same medium as Panel A but containing 100  $\mu$ M Fe.

**Aconitase Activity of *ylaN* Mutant**

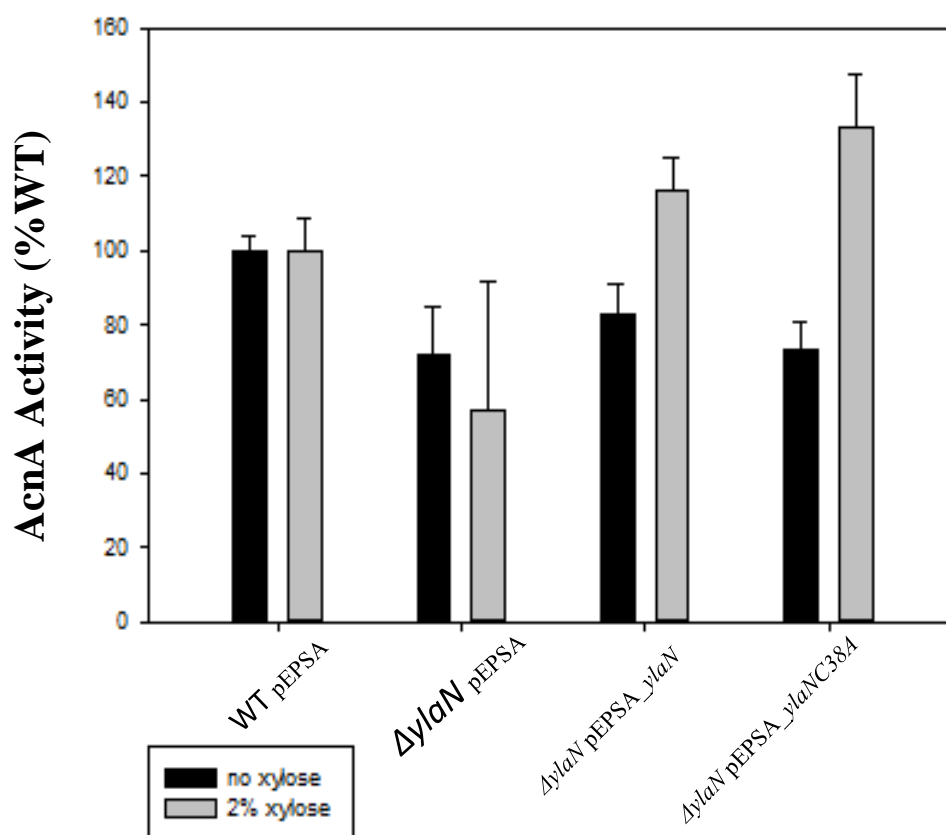


**Aconitase Activity of *ylaN* mutant grown in the presence of 120  $\mu$ M DIP**

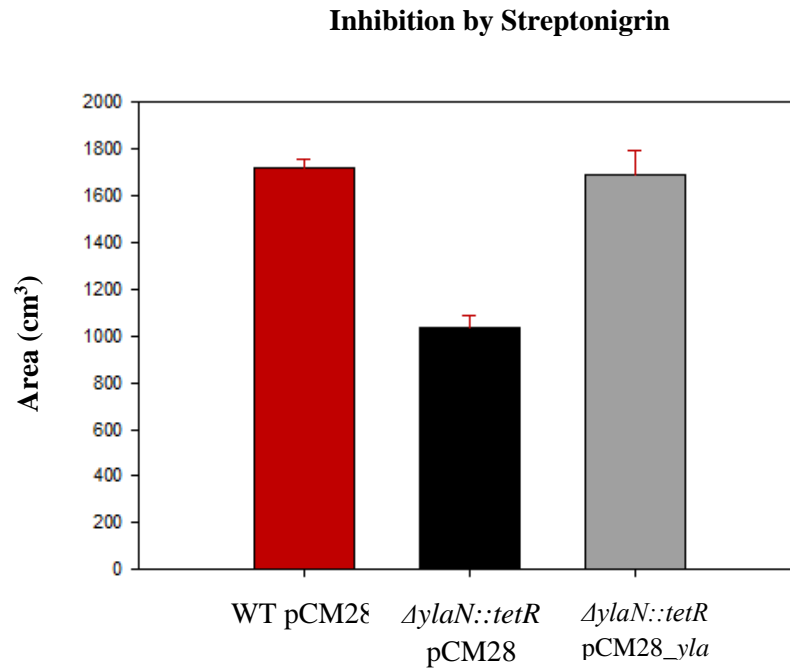


**Figure 3: Aconitase activity of *ylaN*.** Panel A. The activity of aconitase was measured in cell-free lysates from the WT and *ylaN* strains. Panel B. Aconitase activity was determined in cell-free lysates harvested from the *acnA* and *acnA ylaN* strains containing pEPSA\_acynA after growth in TSB with and without 120  $\mu$ M DIP. The data represent the average of biological triplicates with standard deviations shown.

## Aconitase Activity

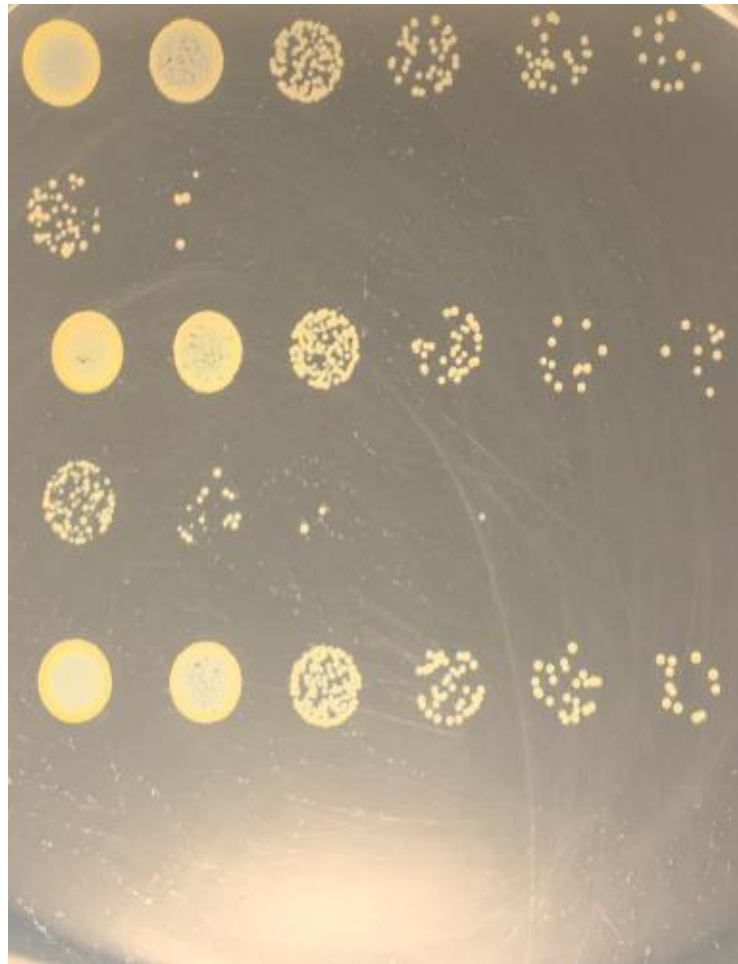


**Figure 4: Aconitase activity of *ΔylaN* with complementation.** *ylaN* and *ylaN<sub>C38A</sub>* were cloned into a complementation plasmid with a xylose inducible promoter and added back into the *ΔylaN* mutant. Aconitase activity was measured with and without plasmid induction. The data represent the average of biological triplicates with standard deviations shown.

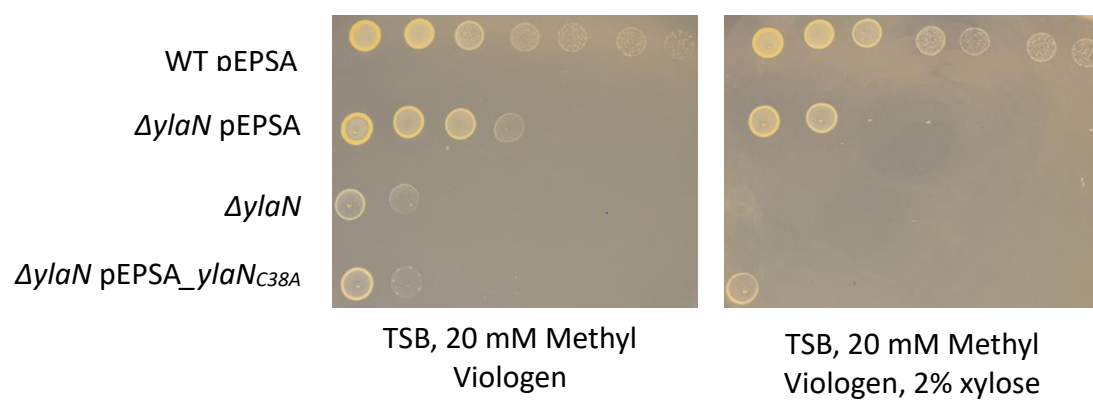


**Figure 5: Growth of  $\Delta ylaN$  treated with streptonigrin.** Top agar overlays containing the WT with pCM28,  $\Delta ylaN::tetR$  with pCM28, or  $\Delta ylaN::tetR$  with pCM28\_yla were plated on TSB containing chloramphenicol. 5  $\mu$ L of 2 mg/mL streptonigrin was spotted on the center of each plate, and the zone of inhibition was determined. The data represent the average of biological triplicates with standard deviations shown.

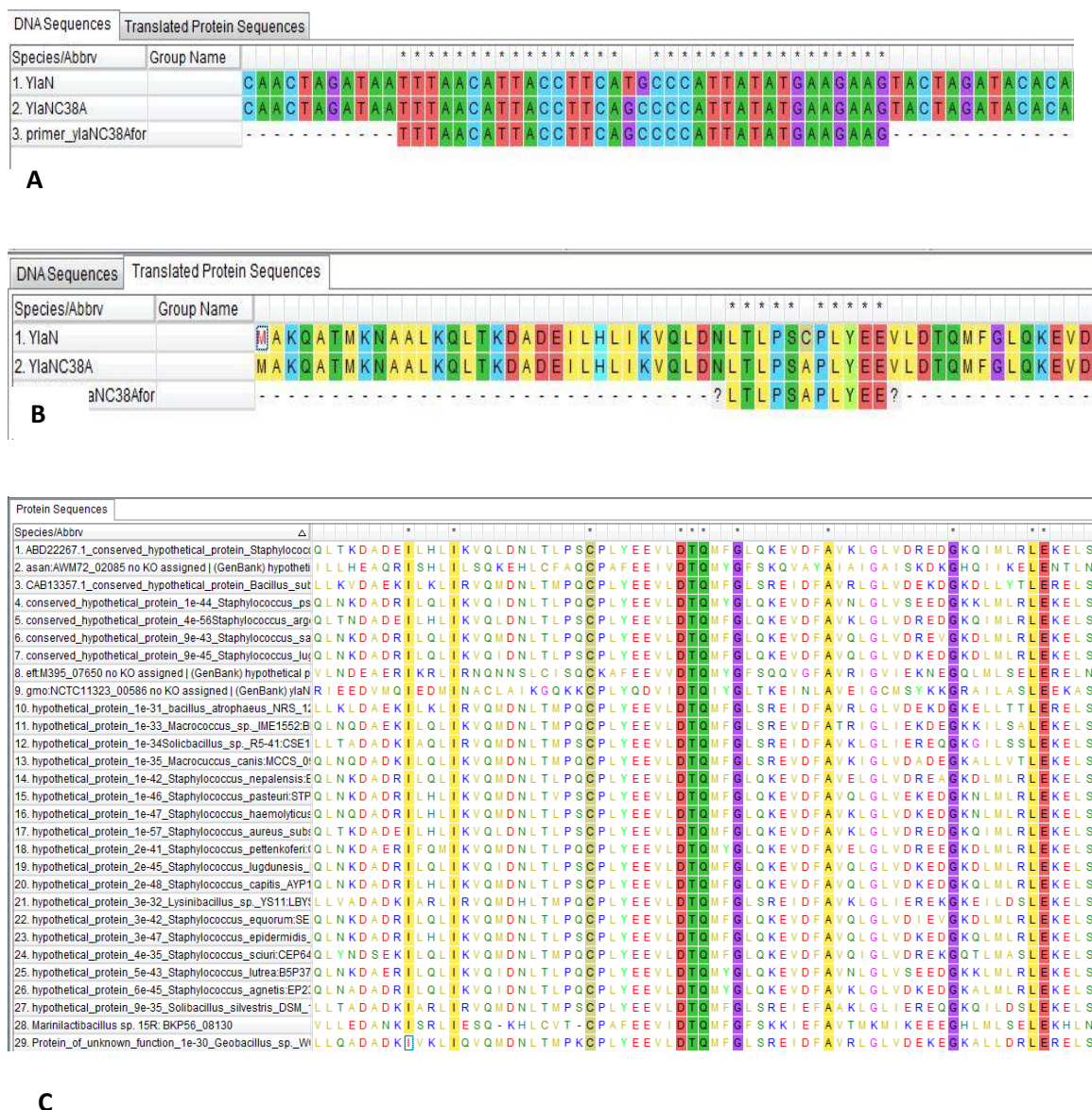
WT

WT + H<sub>2</sub>O<sub>2</sub>*ylaN::tet**ylaN::tet* + H<sub>2</sub>O<sub>2</sub>*Kat::tet**Kat::tet* + H<sub>2</sub>O<sub>2</sub>**H<sub>2</sub>O<sub>2</sub> Assay - 1.5 M H<sub>2</sub>O<sub>2</sub>**

**Figure 6: Survival after treatment with hydrogen peroxide.** The  $\Delta ylaN$  and WT strains were exposed to 1.5 M of H<sub>2</sub>O<sub>2</sub> for two hours, serial diluted, and spot plated on a TSA plate. A  $\Delta kat$  strain that lacks catalase was used as a positive control. A picture of a representative experiment is shown.



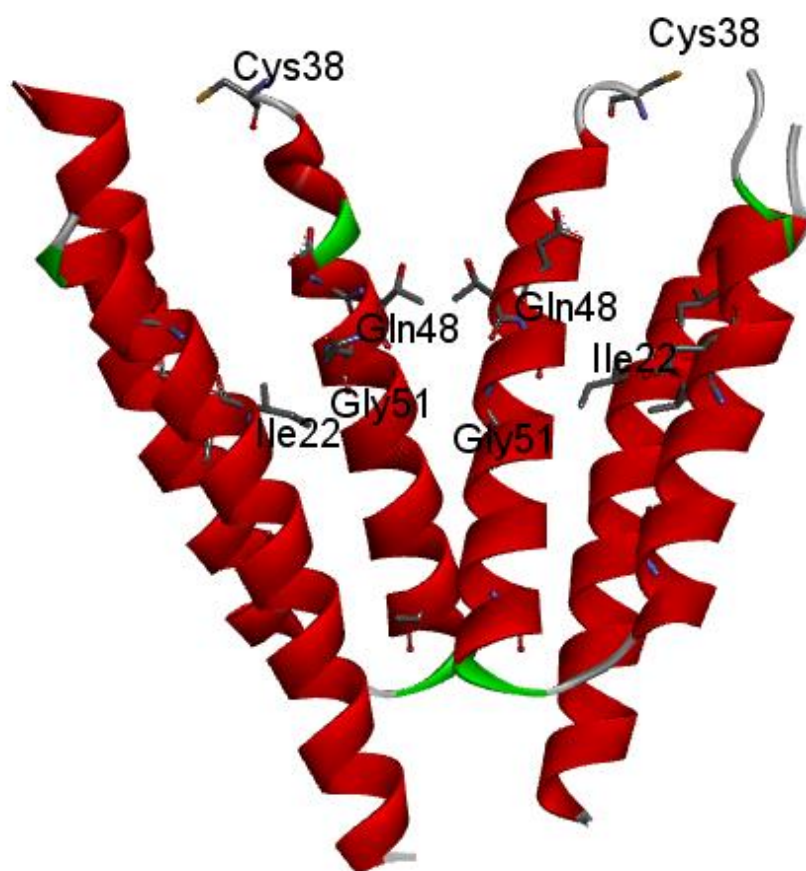
**Figure 7: Growth in the presence of methyl viologen.** WT with pEPSA,  $\Delta ylaN$  with pEPSA,  $\Delta ylaN$  with pEPSA\_ylaN, and  $\Delta ylaN$  with pEPSA\_ylaN<sub>C38A</sub> were plated on TSB containing methyl viologen. A picture of a representative experiment is shown.



**Figure 8: Sequence alignments of YlaN, YlaN<sub>C38A</sub> variant, and YlaN homologs. Panel A.**

DNA sequence alignment of the original *ylaN* sequence, the verified sequence received from GeneWiz of *ylaN*<sub>C38A</sub>, and the forward primer used to make the site-directed mutations 112T>G and 113G>C. Panel B. The amino acid alignment of YlaN, YlaN<sub>C38A</sub>, and the forward primer showing the resulting C38A mutation. Panel C. An amino acid alignment showing 11 conserved residues (highlighted) between 29 YlaN homologs.




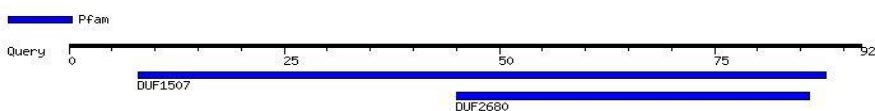


**Figure 9: Protein structure of YlaN homodimer.** Image was created using Dassault Systèmes Biovia, Discovery Studio Visualizer, 2017R2 (Dassault Systèmes, 2017). Protein Data Base, ID: 20DM (Xu et al., 2007). The 11 conserved amino acid residues are shown in line form. The location of the cysteine chosen for site-directed mutagenesis can be seen at the top of each protein (Cys38). Conserved residues Ile22, Gln48, and Gly51 are also labeled for each protein.

## Result of MotifFinder

A

Number of found motifs: 2 



Pfam (2 motifs)

Pfam	Position(Independent E-value)		Description
DUF1507	8..88(1.7e-36)	<a href="#">Detail</a>	PF07408, Protein of unknown function (DUF1507)
DUF2680	45..86(0.0027)	<a href="#">Detail</a>	PF10925, Protein of unknown function (DUF2680)

## Motif in the sequence

B

Pfam ID:

DUF1507

Description:

PF07408, Protein of unknown function (DUF1507)

Appearance:

Position	8..88
Alignment Query Database	KNAALKQLTKDADEILHLIKVQLDNLTPSCPLYEEVLDTQMFGQLKEVDFAVKGLGLVDREDGKQIMLRLEKELSKLHEAF kekalellkedadkikklikvqmdnltlsqCplyEevlDtqmyGlsrevidfavrIgliieeeeGkqllseLekeInqlyeev
i-Value	1.7e-36

Sequence:

MAKQATMKNAALKQLTKDADEILHLIKVQLDNLTPSCPLYEEVLDTQMFGQLKEVDFAV  
KGLGLVDREDGKQIMLRLEKELSKLHEAFTLV

## Motif in the sequence

C

Pfam ID:

DUF2680

Description:

PF10925, Protein of unknown function (DUF2680)

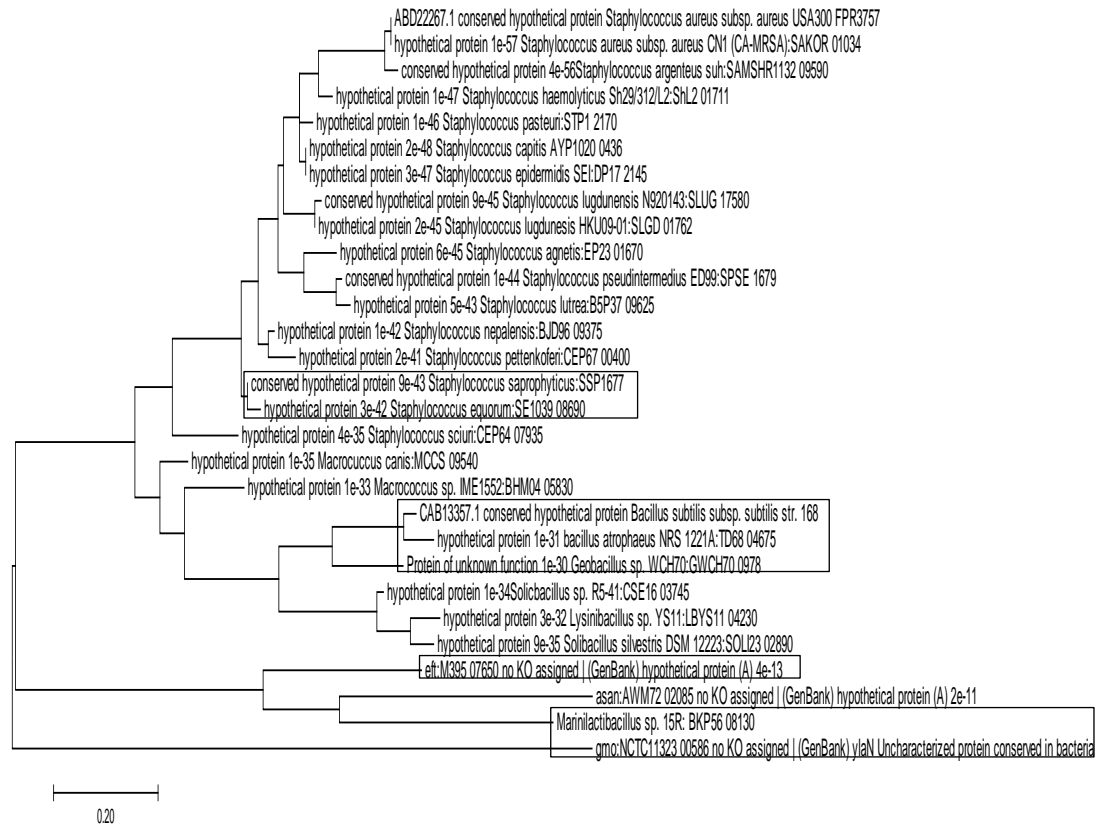
Appearance:

Position	45..86
Alignment Query Database	LDTQMFGQLKE-VDFAVKGLGLVDREDGKQIMLRLEKELSKLHE LyqqiaelrKqivdKyVeaGllTkeqgekikknIDkr1kylke
i-Value	0.0027

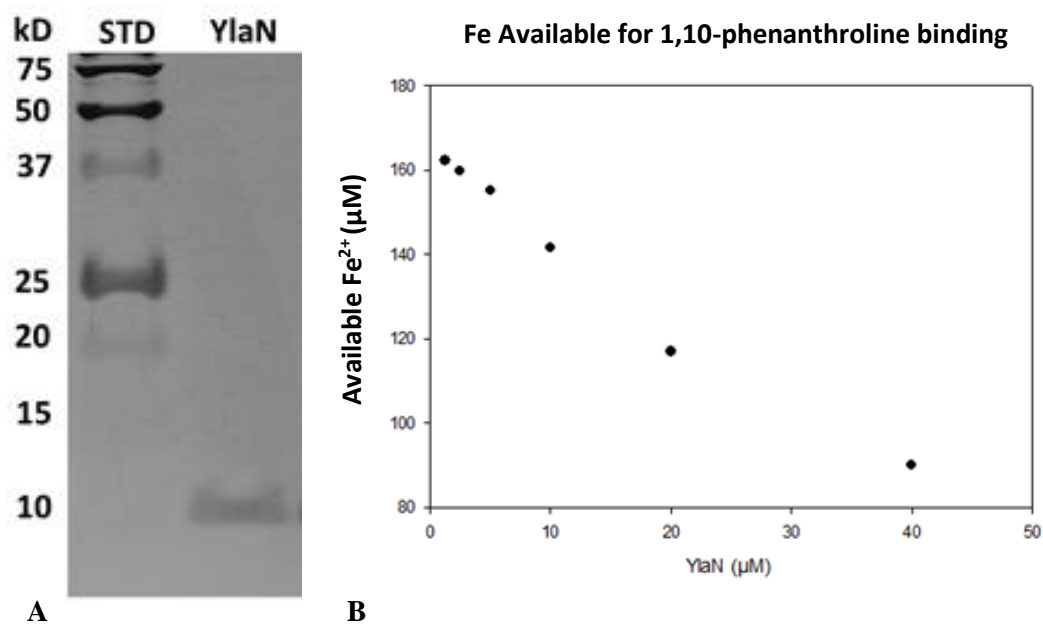
Sequence:

MAKQATMKNAALKQLTKDADEILHLIKVQLDNLTPSCPLYEEVLDTQMFGQLKEVDFAV  
KGLGLVDREDGKQIMLRLEKELSKLHEAFTLV

**Figure 10: Identified domains of YlaN.** Panel A. Results of the motif search using GenomeNet with the YlaN amino acid sequence from *S. aureus* as the input. Two overlapping domains were found; DUF1507 and DUF2680, both with unknown functions. Panel B. The DUF1507 motif spans from amino acid 8 to 88. Panel C. The DUF2680 motif spans amino acids 45-86.

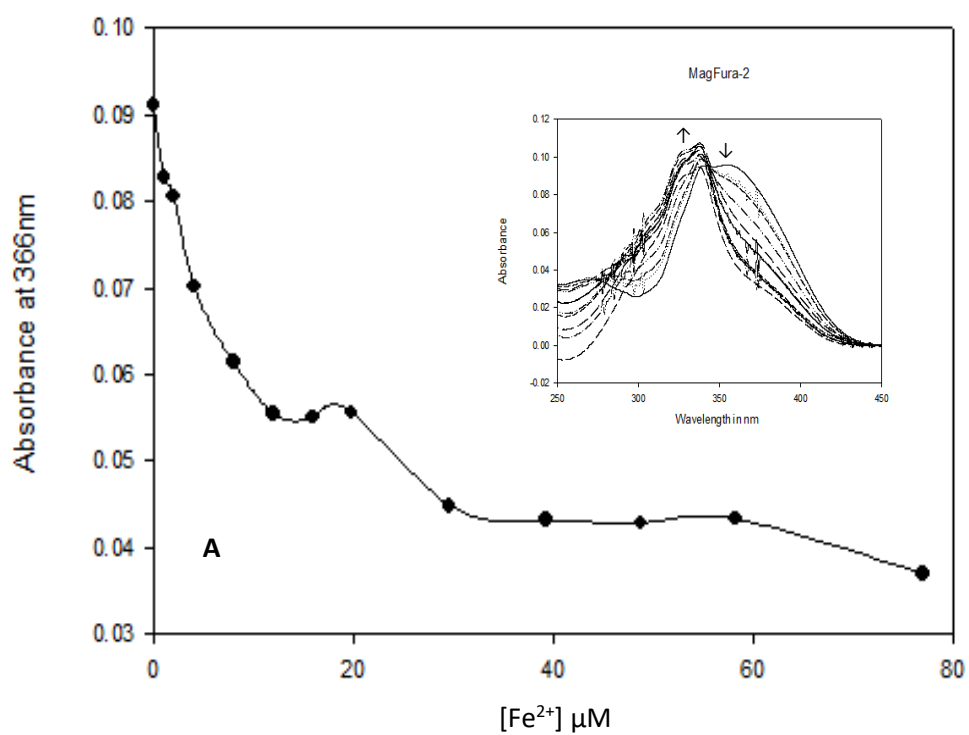


**Figure 11: Maximum likelihood tree for YlaN homologs.** This tree represents the results of a maximum likelihood analysis and shows the tree with the highest log likelihood value ( -1891.8262). Branch lengths are equal to substitutions per site over time. All nodes on the tree have the support of 100%. Sequences enclosed in boxes do not contain the DUF2680 domain. Gaps and missing data were deleted, leaving 86 amino acid positions for the analysis.

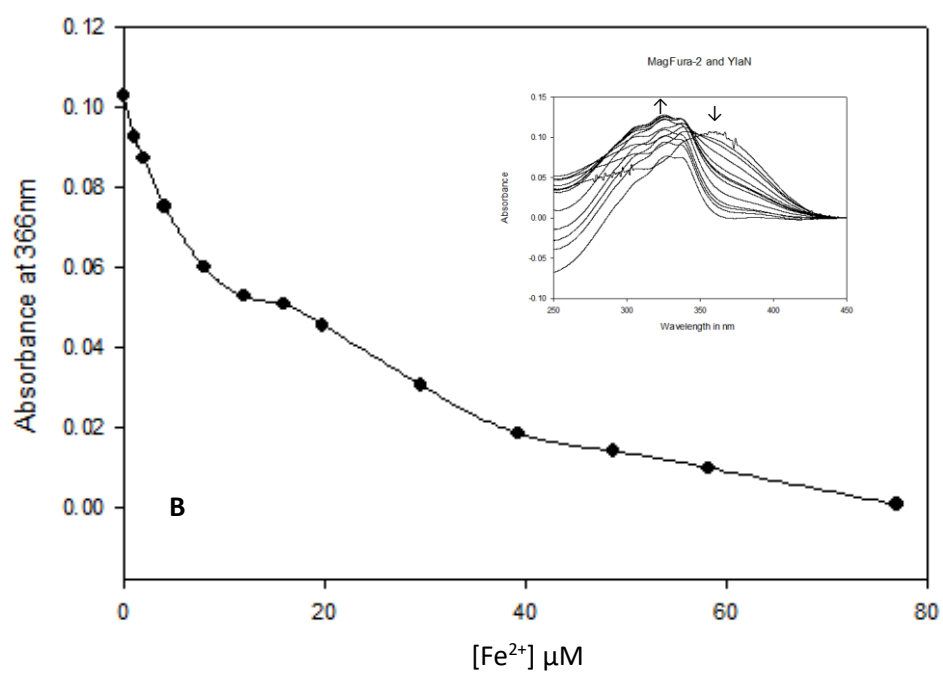


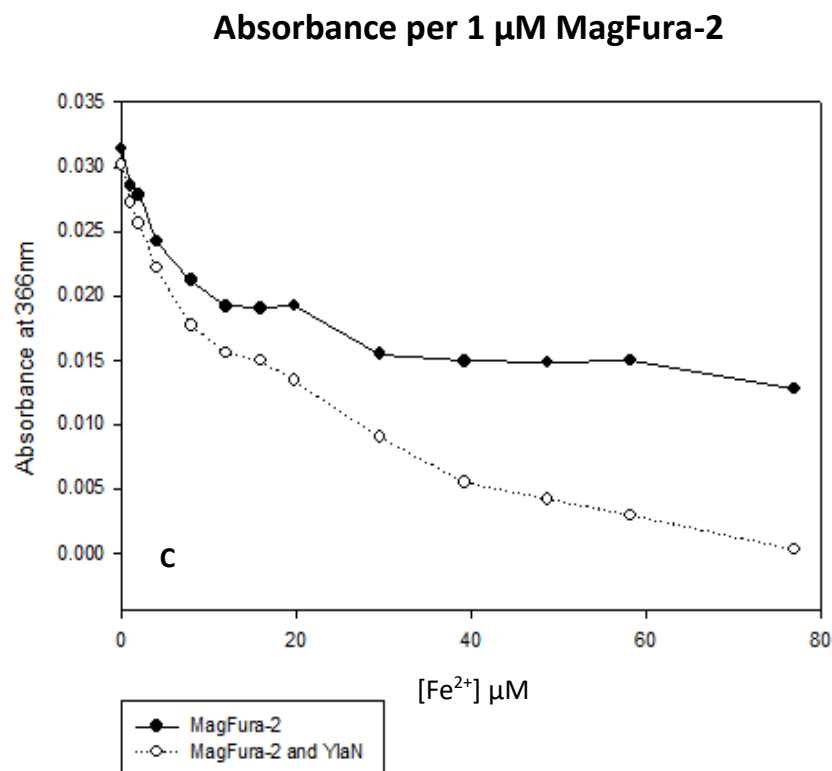
**Figure 12: Fe competition between YlaN and 1,10-phenanthroline.** Panel A. *S. aureus* YlaN purity was verified by SDS-PAGE gel electrophoresis. Panel B. An iron binding competition assay between 1,10-phenanthroline and increasing concentrations of YlaN was performed and analyzed by UV-VIS at a wavelength of 510 nm. The absorbance was converted into available iron.

## MagFura-2



## MagFura-2 and YlaN





**Figure 13: Fe competition between YlaN and MagFura-2.** Panel A. The change in absorbance at 366 nm with increasing Fe<sup>2+</sup> is seen for MagFura-2 in the absence of YlaN. The inset shows the absorbance spectra for MagFura-2 between 250-450 nm. Panel B. The change in absorbance at 366 nm with increasing Fe<sup>2+</sup> is seen for MagFura-2 in the presence of YlaN with. The inset shows the absorbance spectra between 250-450 nm. Panel C. The change in absorbance at 366 nm per 1  $\mu$ M MagFura-2 is shown, in the presence and absence of YlaN.

## References

- A., M.A., A., R.C., Shiven, B., L., M.K., K., C.R., N., S.L., and M., B.J. (2016). *Staphylococcus aureus* SufT: an essential iron-sulphur cluster assembly factor in cells experiencing a high-demand for lipoic acid. *Molecular Microbiology* 102, 1099-1119.
- A., M.A., Y., P.Y., Zuelay, R.-C., K., C.H., A., B.M., A., M.L., P., S.E., J., T.V., M., N.W., and M., B.J. (2015). Nfu facilitates the maturation of iron-sulfur proteins and participates in virulence in *Staphylococcus aureus*. *Molecular Microbiology* 95, 383-409.
- Andrews, S.C., Robinson, A.K., and Rodríguez-Quñones, F. (2003). Bacterial iron homeostasis. *FEMS Microbiology Reviews* 27, 215-237.
- Barbour, S.D., Shlaes, D.M., and Guertin, S.R. (1984). Toxic-shock syndrome associated with nasal packing: analogy to tampon-associated illness. *Pediatrics* 73, 163-165.
- Beinert, H., Holm, R.H., and Münck, E. (1997). Iron-sulfur clusters: nature's modular, multipurpose structures. *Science* 277, 653-659.
- Boles, B.R., Thoendel, M., Roth, A.J., and Horswill, A.R. (2010). Identification of genes involved in polysaccharide-independent *Staphylococcus aureus* biofilm formation. *PloS One* 5, e10146.
- Bose, J.L., Fey, P.D., and Bayles, K.W. (2013). Genetic tools to enhance the study of gene function and regulation in *Staphylococcus aureus*. *Applied and Environmental Microbiology*, 00136-00113.
- Boyd, E.S., Thomas, K.M., Dai, Y., Boyd, J.M., and Outten, F.W. (2014). Interplay between oxygen and Fe-S cluster biogenesis: insights from the Suf pathway. *Biochemistry* 53, 5834-5847.
- Bus, J.S., and Gibson, J.E. (1984). Paraquat: model for oxidant-initiated toxicity. *Environmental Health Perspectives* 55, 37.
- Cabiscol Català, E., Tamarit Sumalla, J., and Ros Salvador, J. (2000). Oxidative stress in bacteria and protein damage by reactive oxygen species. *International Microbiology*, 2000, vol 3, núm 1, p 3-8.
- Cassat, J.E., and Skaar, E.P. (2013). Iron in infection and immunity. *Cell Host & Microbe* 13, 509-519.
- Choby, J.E., Mike, L.A., Mashruwala, A.A., Dutter, B.F., Dunman, P.M., Sulikowski, G.A., Boyd, J.M., and Skaar, E.P. (2016). A small-molecule inhibitor of iron-sulfur cluster assembly uncovers a link between virulence regulation and metabolism in *Staphylococcus aureus*. *Cell Chemical Biology* 23, 1351-1361.
- Cohen, M., Chai, Y., Britigan, B., McKenna, W., Adams, J., Svendsen, T., Bean, K., Hassett, D., and Sparling, P. (1987). Role of extracellular iron in the action of the quinone antibiotic streptonigrin: mechanisms of killing and resistance of *Neisseria gonorrhoeae*. *Antimicrobial Agents and Chemotherapy* 31, 1507-1513.

Dassault Systèmes Biovia, Discovery Studio Visualizer, 2017R2, San Diego: Dassault Systèmes, 2017.

Forsyth, R.A., Haselbeck, R.J., Ohlsen, K.L., Yamamoto, R.T., Xu, H., Trawick, J.D., Wall, D., Wang, L., Brown-Driver, V., and Froelich, J.M. (2002). A genome-wide strategy for the identification of essential genes in *Staphylococcus aureus*. *Molecular Microbiology* 43, 1387-1400.

Frey, A.G., Nandal, A., Park, J.H., Smith, P.M., Yabe, T., Ryu, M.-S., Ghosh, M.C., Lee, J., Rouault, T.A., and Park, M.H. (2014). Iron chaperones PCBP1 and PCBP2 mediate the metallation of the dinuclear iron enzyme deoxyhypusine hydroxylase. *Proceedings of the National Academy of Sciences*, 201402732.

Hantke, K. (1981). Regulation of ferric iron transport in *Escherichia coli* K12: isolation of a constitutive mutant. *Molecular and General Genetics* 182, 288-292.

Hantke, K. (2001). Iron and metal regulation in bacteria. *Current Opinion in Microbiology* 4, 172-177.

Hassan, H.M., and Fridovich, I. (1977). Physiological function of superoxide dismutase in glucose-limited chemostat cultures of *Escherichia coli*. *Journal of Bacteriology* 130, 805-811.

Hirling, H., Henderson, B., and Kühn, L. (1994). Mutational analysis of the [4Fe-4S]-cluster converting iron regulatory factor from its RNA-binding form to cytoplasmic aconitase. *The EMBO Journal* 13, 453-461.

Hong, J.S., Champion, A., and Rabinowitz, J. (1969). Concerning the Source of “Labile” Sulfur in Clostridial Ferredoxin. *European Journal of Biochemistry* 8, 307-313.

Horbach, S., Sahm, H., and Welle, R. (1993). Isoprenoid biosynthesis in bacteria: two different pathways? *FEMS Microbiology Letters* 111, 135-140.

Horsburgh, M.J., Ingham, E., and Foster, S.J. (2001). In *Staphylococcus aureus*, fur is an interactive regulator with PerR, contributes to virulence, and is necessary for oxidative stress resistance through positive regulation of catalase and iron homeostasis. *Journal of Bacteriology* 183, 468-475.

Huber, C., and Wächtershäuser, G. (1997). Activated acetic acid by carbon fixation on (Fe, Ni) S under primordial conditions. *Science* 276, 245-247.

Jang, S., and Imlay, J.A. (2007). Micromolar intracellular hydrogen peroxide disrupts metabolism by damaging iron-sulfur enzymes. *Journal of Biological Chemistry* 282, 929-937.

Jones, D.T., Taylor, W.R., and Thornton, J.M. (1992). The rapid generation of mutation data matrices from protein sequences. *Bioinformatics* 8, 275-282.

Joska, T.M., Mashruwala, A., Boyd, J.M., and Belden, W.J. (2014). A universal cloning method based on yeast homologous recombination that is simple, efficient, and versatile. *Journal of Microbiological Methods* 100, 46-51.



Kanehisa, M., Goto, S., Kawashima, S., and Nakaya, A. (2002). The KEGG databases at GenomeNet. *Nucleic Acids Research* 30, 42-46.

Kennedy, M., and Beinert, H. (1988a). The state of cluster SH and S2-of aconitase during cluster interconversions and removal. A convenient preparation of apoenzyme. *Journal of Biological Chemistry* 263, 8194-8198.

Kennedy, M.C., and Beinert, H. (1988b). The state of cluster SH and S2- of aconitase during cluster interconversions and removal. A convenient preparation of apoenzyme. *Journal of Biological Chemistry* 263, 8194-8198.

Kennedy, M.C., Emptage, M., Dreyer, J.-L., and Beinert, H. (1983). The role of iron in the activation-inactivation of aconitase. *Journal of Biological Chemistry* 258, 11098-11105.

Keyer, K., and Imlay, J.A. (1996). Superoxide accelerates DNA damage by elevating free-iron levels. *Proceedings of the National Academy of Sciences* 93, 13635-13640.

Koshima, H. (1986). Adsorption of iron (III), gold (III), gallium (III), thallium (III) and antimony (V) on Amberlite XAD and Chelex 100 resins from hydrochloric acid solution. *Analytical Sciences* 2, 255-260.

Kreiswirth, B.N., Löfdahl, S., Betley, M.J., O'Reilly, M., Schlievert, P.M., Bergdoll, M.S., and Novick, R.P. (1983). The toxic shock syndrome exotoxin structural gene is not detectably transmitted by a prophage. *Nature* 305, 709.

Kuehnert, M.J., Kruszon-Moran, D., Hill, H.A., McQuillan, G., McAllister, S.K., Fosheim, G., McDougal, L.K., Chaitram, J., Jensen, B., Fridkin, S.K., *et al.* (2006). Prevalence of *Staphylococcus aureus* Nasal Colonization in the United States, 2001–2002. *The Journal of Infectious Diseases* 193, 172-179.

Kumar, S., Stecher, G., and Tamura, K. (2016). MEGA7: molecular evolutionary genetics analysis version 7.0 for bigger datasets. *Molecular biology and evolution* 33, 1870-1874.

Laulhère, J.P., Labouré, A.M., Van Wuytswinkel, O., Gagnon, J., and Briat, J.F. (1992). Purification, characterization and function of bacterioferritin from the cyanobacterium *Synechocystis* P.C.C. 6803. *Biochemical Journal* 281, 785-793.

Lee, T.S., Kolthoff, I.M., and Leussing, D.L. (1948). Reaction of Ferrous and Ferric Iron with 1,10-Phenanthroline. I. Dissociation Constants of Ferrous and Ferric Phenanthroline. *Journal of the American Chemical Society* 70, 2348-2352.

Lill, R. (2009). Function and biogenesis of iron–sulphur proteins. *Nature* 460, 831.

Ling, X., E., S.S., J., B.P., Alison, H., Jeff, E., and W., R.D. (2007). Crystal structure of *S. aureus* YlaN, an essential leucine rich protein involved in the control of cell shape. *Proteins: Structure, Function, and Bioinformatics* 68, 438-445.

Mashruwala, A.A., Bhatt, S., Poudel, S., Boyd, E.S., and Boyd, J.M. (2016). The DUF59 Containing Protein SufT Is Involved in the Maturation of Iron-Sulfur (FeS) Proteins during Conditions of High FeS Cofactor Demand in *Staphylococcus aureus*. *PLOS Genetics* 12, e1006233.

- Miller, L.G., Perdreau-Remington, F., Rieg, G., Mehdi, S., Perlroth, J., Bayer, A.S., Tang, A.W., Phung, T.O., and Spellberg, B. (2005). Necrotizing Fasciitis Caused by Community-Associated Methicillin-Resistant *Staphylococcus aureus* in Los Angeles. *New England Journal of Medicine* 352, 1445-1453.
- Nao, Y., Chihiro, N., Yukari, O., Masaharu, S., Takuya, T., Wen, C., Kotomi, S., Chihiro, M., Takuya, S., Eiki, Y., *et al.* (2018). Distinct roles for U-type proteins in iron–sulfur cluster biosynthesis revealed by genetic analysis of the *Bacillus subtilis* sufCDSUB operon. *Molecular Microbiology* 107, 688-703.
- Naoyuki, T., Miaki, K., Keitaro, T., Nao, Y., Tomohisa, K., and Yasuhiro, T. (2016). Novel features of the ISC machinery revealed by characterization of *Escherichia coli* mutants that survive without iron–sulfur clusters. *Molecular Microbiology* 99, 835-848.
- Niederhoffer, E.C., Naranjo, C.M., Bradley, K.L., and Fee, J.A. (1990). Control of *Escherichia coli* superoxide dismutase (sodA and sodB) genes by the ferric uptake regulation (fur) locus. *Journal of Bacteriology* 172, 1930-1938.
- Pang, Y.Y., Schwartz, J., Thoendel, M., Ackermann, L.W., Horswill, A.R., and Nauseef, W.M. (2010). agr-Dependent Interactions of *Staphylococcus aureus* USA300 with Human Polymorphonuclear Neutrophils. *Journal of Innate Immunity* 2, 546-559.
- Peck, S.C., and van der Donk, W.A. (2017). Go it alone: four-electron oxidations by mononuclear non-heme iron enzymes. *Journal of Biological Inorganic Chemistry* 22, 381-394.
- Peters, J.M., Colavin, A., Shi, H., Czarny, T.L., Larson, M.H., Wong, S., Hawkins, J.S., Lu, C.H.S., Koo, B.-M., Marta, E., *et al.* (2016). A Comprehensive, CRISPR-based Functional Analysis of Essential Genes in Bacteria. *Cell* 165, 1493-1506.
- Roberts, C.A., Al-Tameemi, H.M., Mashruwala, A.A., Rosario-Cruz, Z., Chauhan, U., Sause, W.E., Torres, V.J., Belden, W.J., and Boyd, J.M. (2017). The Suf Iron-Sulfur Cluster Biosynthetic System Is Essential in *Staphylococcus aureus*, and Decreased Suf Function Results in Global Metabolic Defects and Reduced Survival in Human Neutrophils. *Infection and Immunity* 85, e00100-00117.
- Rodrigues, A.V., Kandegedara, A., Rotondo, J.A., Dancis, A., and Stemmler, T.L. (2015). Iron loading site on the Fe–S cluster assembly scaffold protein is distinct from the active site. *BioMetals* 28, 567-576.
- Skaar, E.P. (2010). The Battle for Iron between Bacterial Pathogens and Their Vertebrate Hosts. *PLOS Pathogens* 6, e1000949.
- Takahashi, Y., and Tokumoto, U. (2002). A Third Bacterial System for the Assembly of Iron-Sulfur Clusters with Homologs in Archaea and Plastids. *Journal of Biological Chemistry* 277, 28380-28383.
- Tardat, B., and Touati, D. (1991). Two global regulators repress the anaerobic expression of MnSOD in *Escherichia coli*: Fur (ferric uptake regulation) and Arc (aerobic respiration control). *Molecular microbiology* 5, 455-465.

- Tong, S.Y.C., Davis, J.S., Eichenberger, E., Holland, T.L., and Fowler, V.G. (2015). *Staphylococcus aureus* Infections: Epidemiology, Pathophysiology, Clinical Manifestations, and Management. *Clinical Microbiology Reviews* 28, 603-661.
- Valentino, M.D., Foulston, L., Sadaka, A., Kos, V.N., Villet, R.A., Santa Maria, J., Lazinski, D.W., Camilli, A., Walker, S., Hooper, D.C., *et al.* (2014). Genes Contributing to *Staphylococcus aureus* Fitness in Abscess- and Infection-Related Ecologies. *mBio* 5.
- Wagner, W.P., Helmig, D., and Fall, R. (2000). Isoprene Biosynthesis in *Bacillus subtilis* via the Methylerythritol Phosphate Pathway. *Journal of Natural Products* 63, 37-40.
- Wayne, O.F., Ouliana, D., and Gisela, S. (2004). A suf operon requirement for Fe–S cluster assembly during iron starvation in *Escherichia coli*. *Molecular Microbiology* 52, 861-872.
- Weixue, W., and Eric, O. (2014). Bioorganometallic Chemistry with IspG and IspH: Structure, Function, and Inhibition of the [Fe<sub>4</sub>S<sub>4</sub>] Proteins Involved in Isoprenoid Biosynthesis. *Angewandte Chemie International Edition* 53, 4294-4310.
- Williams, P.H., and Carbonetti, N.H. (1986). Iron, siderophores, and the pursuit of virulence: independence of the aerobactin and enterochelin iron uptake systems in *Escherichia coli*. *Infection and Immunity* 51, 942-947.
- Yaroshevsky, A.A. (2006). Abundances of chemical elements in the Earth's crust. *Geochemistry International* 44, 48-55.
- Yasmin, S., Andrews, S.C., Moore, G.R., and LeBrun, N.E. (2010). A new role for heme: facilitating release of iron from the bacterioferritin iron biomineral. *Journal of Biological Chemistry* 286, 3473-3483.
- Yeowell, H.N., and White, J.R. (1982). Iron requirement in the bactericidal mechanism of streptonigrin. *Antimicrobial Agents and Chemotherapy* 22, 961-968.
- Zheng, L., Cash, V.L., Flint, D.H., and Dean, D.R. (1998). Assembly of Iron-Sulfur Clusters: IDENTIFICATION OF AN iscSUA-hscBA-fdx GENE CLUSTER FROM AZOTOBACTER VINELANDII. *Journal of Biological Chemistry* 273, 13264-13272.
- Zheng, L., White, R.H., Cash, V.L., Jack, R.F., and Dean, D.R. (1993). Cysteine desulfurase activity indicates a role for NIFS in metallocluster biosynthesis. *Proceedings of the National Academy of Sciences* 90, 2754-2758.
- Zuelay, R.-C., K., C.H., A., M.L., P., S.E., and M., B.J. (2015). Bacillithiol has a role in Fe–S cluster biogenesis in *Staphylococcus aureus*. *Molecular Microbiology* 98, 218-242.